

Analysis of Fourier Neural Operators via Effective Field Theory

Taeyoung Kim

*School of Computational Sciences
Korea Institute for Advanced Study
Seoul 02455, South Korea*

TAEYOUNGKIM@KIAS.RE.KR

Abstract

Fourier Neural Operators (FNOs) have emerged as leading surrogates for high-dimensional partial-differential equations, yet their stability, generalization and frequency behavior lack a principled explanation. We present the first systematic effective-field-theory analysis of FNOs in an infinite-dimensional function space, deriving closed recursion relations for the layer kernel and four-point vertex and then examining three practically important settings-analytic activations, scale-invariant cases and architectures with residual connections. The theory shows that nonlinear activations inevitably couple frequency inputs to high-frequency modes that are otherwise discarded by spectral truncation, and experiments confirm this frequency transfer. For wide networks we obtain explicit criticality conditions on the weight-initialization ensemble that keep small input perturbations to have uniform scale across depth, and empirical tests validate these predictions. Taken together, our results quantify how nonlinearity enables neural operators to capture non-trivial features, supply criteria for hyper-parameter selection via criticality analysis, and explain why scale-invariant activations and residual connections enhance feature learning in FNOs.

Keywords: Neural Operators, Deep Learning Theory, Effective Field Theory

1. Introduction

1.1 Fourier Neural Operator

In scientific machine learning, neural operators—networks that approximate solution operators so they can act directly on functional data—are attracting growing attention (Kovachki et al. (2021b), Lu et al. (2021)). In addition to the linear layers of standard fully connected networks (FCNs), neural-operator architectures include layers that approximate a kernel and apply an integral transform. How the kernel is represented gives rise to many variants: graph-based constructions (Li et al. (2020)), tensor-product decompositions (Kovachki et al. (2021b)), hierarchical (multi-resolution) kernels (Gupta et al. (2021)), and, most notably, Fourier Neural Operators (FNOs) (Li et al. (2021)). Thanks to their computational efficiency, high accuracy, and ability to capture long-range interactions that elude CNNs and GNNs, FNOs have become the workhorse choice for surrogate modeling (Pathak et al. (2022), Sun et al. (2023)). Prior theory has addressed their generalization error (Kim and Kang (2024), Benitez et al. (2024)), universal approximation property (Kovachki et al. (2021a), Lee et al. (2025)), and expressivity/trainability from a mean-field perspective (Koshizuka et al. (2024)), yet a comprehensive statistical description is still lacking. Here we fill that gap by analysing FNOs through the lens of effective field theory (EFT).

1.2 Effective Field Theory for Neural Networks

Because stochastic elements such as random initialisation and stochastic gradient descent are intrinsic to neural networks, statistical-physics tools are natural candidates for theoretical analysis. Recent work has imported methods from field theory (Halverson et al. (2021), Banta et al. (2024)), relating connected correlators in randomly initialised ensembles and deriving susceptibility-based criticality conditions that predict when training remains stable (Roberts et al. (2022)). Within the EFT framework one can see how the choice of activation or hyper-parameters moves a model between different universality classes, revealing when signals explode, vanish, or propagate cleanly.

1.3 Contributions

Building on the EFT formulation for FCNs, we extend the approach to Fourier Neural Operators—an essential step, because FNOs act on infinite-dimensional function spaces rather than finite-dimensional vectors. While the basic relations among connected correlators mirror those in FCNs, the architectural differences introduce qualitatively new phenomena: the observables become functions rather than scalars, and mechanisms such as frequency coupling appear. Our analysis quantifies how non-trivial activations and residual connections influence information flow in FNOs and yields explicit design criteria for stable, high-performance models.

2. Preliminary

In this section, we examine the definition of neural operators designed for processing functional data, and explore effective field theory along with its application to the statistical analysis of basic neural networks (fully connected networks). Henceforth, Einstein summation convention will be adopted for repeated indices.

2.1 Effective Field Theory

Suppose that the distribution $p(X_1, \dots, X_n) \sim \exp(-S(X_1, \dots, X_n))$ is given. For an analytic function $f(x_1, \dots, x_n) = \sum a_{i_1 \dots i_n} x_1^{i_1} \dots x_n^{i_n}$ the expectation of f with respect to p is expressed as

$$\mathbb{E}[f(X_1, \dots, X_n)] = \sum a_{i_1 \dots i_n} \mathbb{E}[X_1^{i_1} \dots X_n^{i_n}]$$

Thus, in the analytic observable case, the collection of terms $\mathbb{E}[X_1^{i_1} \dots X_n^{i_n}]$ contains all the information about the distribution. These terms are referred to as the $(i_1 + \dots + i_n)$ -point correlators (or $(i_1 + \dots + i_n)$ -th moments). For a Gaussian distribution, where $S(X_1, \dots, X_n)$ consists solely of quadratic terms, the following well-known result holds:

Proposition 1 (Wick contraction) Suppose (X_1, \dots, X_n) is a zero-mean multivariate normal random vector. Then, all odd-order correlators vanish, and the even-order correlators are given by

$$\mathbb{E}[X_{j_1}^{i_1} \dots X_{j_n}^{i_n}] = \sum_{(\text{all possible pairings})} \prod_{(\text{pairings})} \mathbb{E}[X_{p_1} X_{p_2}]$$

Motivated by this proposition, we define the connected correlator (or cumulant) for an arbitrary distribution as follows:

Definition 1 The k -point connected correlator (or k -th cumulant, $k = i_1 + \dots + i_n$) is defined by

$$\begin{aligned} \mathbb{E}|_{\text{conn}}[X_{j_1}^{i_1} \dots X_{j_n}^{i_n}] &:= \mathbb{E}[X_{j_1}^{i_1} \dots X_{j_n}^{i_n}] \\ &- \sum_{\substack{\text{all subdivisions of } (1, \dots, 2k)}} \mathbb{E}[X_{i_{\mu_1,1}} \dots X_{i_{\mu_1,t_1}}]|_{\text{conn}} \dots \mathbb{E}[X_{i_{\mu_\nu,1}} \dots X_{i_{\mu_\nu,t_\nu}}]|_{\text{conn}} \end{aligned} \quad (1)$$

Since the connected correlators vanish for Gaussian distributions, they serve as an indicator of the deviation of a distribution from Gaussianity. Next, we define the fully connected network (FCN), a basic architecture in deep learning models:

Definition 2 The FCN is composed as follows:

$$\begin{aligned} z_i^{(1)} &:= \sum_{j=1}^{n_0} W_{ij}^{(1)} x_j + b_i^{(1)} \\ z_i^{(l+1)} &:= \sum_{j=1}^{n_l} W_{ij}^{(l+1)} \sigma(z_j^{(l)}) + b_i^{(l+1)}, \quad l = 1, \dots, L-1. \end{aligned}$$

where $\sigma : \mathbb{R} \rightarrow \mathbb{R}$ is an activation function and x is input-vector, $W^{(l)}, b^{(l)}$ s are weights and biases parameters. $z^{(l)}$ denotes the **preactivation at the l -th layer**.

In deep learning architectures, the learning process involves optimizing the parameters $\{W^{(l)}, b^{(l)}\}_{l=1, \dots, L}$. The initial setting of these parameters, known as **initialization**, follows a specific probability distribution called the **initialization distribution**. For the statistical analysis of neural network preactivations, we assume that the initialization distribution consists of independent and identically distributed (i.i.d.) Gaussian random variables. Specifically, we assume:

$$\begin{aligned} W_{ij}^{(l)} &\sim N\left(0, \frac{C_W}{n_{l-1}}\right) \\ b_i^{(l)} &\sim N(0, C_b). \end{aligned}$$

Then, the statistics of first-layer preactivation is also i.i.d Gaussian distribution with following covariances:

$$\mathbb{E}[z_{i_1; \alpha_1}^{(1)} z_{i_2; \alpha_2}^{(1)}] = \delta_{i_1 i_2} G_{\alpha_1 \alpha_2}^{(1)}$$

where the indices α_j are labels for input data, and $G_{\alpha_1 \alpha_2}^{(1)}$ is a metric for the first preactivation, which contains all the information about the statistics. (since first preactivation is Gaussian)

$$G_{\alpha_1 \alpha_2}^{(1)} = C_b^{(1)} + \frac{C_W^{(1)}}{n_0} \sum_j x_{j; \alpha_1} x_{j; \alpha_2}.$$

Now, the distribution of l -th layer preactivation conditioned on $l-1$ -th layer is also following Gaussian distribution:

$$\mathbb{E}[z_{i_1; \alpha_1}^{(l+1)} z_{i_2; \alpha_2}^{(l+1)} | z^{(l)}] = \delta_{i_1 i_2} \hat{G}_{\alpha_1 \alpha_2}^{(l)}$$

where $\hat{G}_{\alpha_1\alpha_2}^{(l)}$ itself is a random variable, and defined as follows:

$$\hat{G}_{\alpha_1\alpha_2}^{(l)} = C_b^{(l)} + \frac{C_W^{(l)}}{n_{l-1}} \sum_j^{n_l} z_{j;\alpha_1}^{(l-1)} z_{j;\alpha_2}^{(l-1)}.$$

Let the fluctuation of $\hat{G}_{\alpha_1\alpha_2}^{(l)}$ around its mean $G_{\alpha_1\alpha_2}^{(l)} := \mathbb{E}[\hat{G}_{\alpha_1\alpha_2}^{(l)}]$ be $\Delta\hat{G}_{\alpha_1\alpha_2}^{(l)} := \hat{G}_{\alpha_1\alpha_2}^{(l)} - G_{\alpha_1\alpha_2}^{(l)}$ then it can be shown that the variance of this fluctuation is related to 4-point connected correlator and is $\mathcal{O}\left(\frac{1}{n_{l-1}}\right)$. Specifically, we define 4-point vertex as follows:

$$V_{(\alpha_1\alpha_2)(\alpha_3\alpha_4)}^{(l)} := n_{l-1} \mathbb{E}[\Delta\hat{G}_{\alpha_1\alpha_2}^{(l)} \Delta\hat{G}_{\alpha_3\alpha_4}^{(l)}].$$

It can be easily checked that $2k$ -point connected correlators is $\mathcal{O}\left(\frac{1}{n_l^k}\right)$. So, for large enough widths, we can consider the neural network ensembles as a Gaussian processes. As widths go to infinity, the 2-point correlations go to some fixed kernel let denote this kernel as $K_{\alpha_1\alpha_2}^{(l)}$. According to Roberts et al. (2022), for infinite width neural networks, the running of kernels and 4-points vertices are described as follows:

$$\begin{aligned} K_{\alpha_1\alpha_2}^{(l+1)} &= C_b^{(l+1)} + C_W^{(l+1)} \langle \sigma_{\alpha_1} \sigma_{\alpha_2} \rangle_{K^{(l)}}, \\ V_{(\alpha_1\alpha_2)(\alpha_3\alpha_4)}^{(l+1)} &= (C_W^{(l+1)})^2 [\langle \sigma_{\alpha_1} \sigma_{\alpha_2} \sigma_{\alpha_3} \sigma_{\alpha_4} \rangle_{K^{(l)}} - \langle \sigma_{\alpha_1} \sigma_{\alpha_2} \rangle_{K^{(l)}} - \langle \sigma_{\alpha_3} \sigma_{\alpha_4} \rangle_{K^{(l)}}] \\ &\quad + \frac{n_l}{4n_{l-1}} (C_W^{(l+1)})^2 \sum_{\beta_1, \dots, \beta_4 \in \mathcal{D}} V_{(l)}^{(\beta_1\beta_2)(\beta_3\beta_4)} \langle \sigma_{\alpha_1} \sigma_{\alpha_2} (z_{\beta_1} z_{\beta_2} - K_{\beta_1\beta_2}^{(l)}) \rangle_{K^{(l)}} \quad (2) \\ &\quad \langle \sigma_{\alpha_3} \sigma_{\alpha_4} (z_{\beta_3} z_{\beta_4} - K_{\beta_3\beta_4}^{(l)}) \rangle_{K^{(l)}} + \mathcal{O}\left(\frac{1}{n_l}\right) \end{aligned}$$

Let's now examine how the kernel changes under a small perturbation around a reference input x_0 . Define two perturbed inputs $x_{\pm} = x_0 \pm \frac{1}{2}\delta x$, and let $z_{\pm}^{(l)}$ denote their preactivations at layer l . For this two-point dataset, the kernel admits an expansion of the form:

$$K_{\alpha\beta}^{(l)} = \begin{pmatrix} K_{++}^{(l)} & K_{+-}^{(l)} \\ K_{-+}^{(l)} & K_{--}^{(l)} \end{pmatrix} = K_{00}^{(l)} \begin{pmatrix} 1 & 1 \\ 1 & 1 \end{pmatrix} + K_{\parallel}^{(l)} \begin{pmatrix} 1 & 0 \\ 0 & -1 \end{pmatrix} + K_{\perp}^{(l)} \begin{pmatrix} 1 & -1 \\ -1 & 1 \end{pmatrix}.$$

where the coefficients are as follows:

$$\begin{aligned} K_{00}^{(l)} &= \mathbb{E}\left[\frac{1}{n_l} \sum_i^{n_l} x_{i;0}^2\right], \\ K_{\parallel}^{(l)} &= \frac{1}{2} \left(\mathbb{E}\left[\frac{1}{n_l} \sum_i^{n_l} x_{+;0}^2\right] - \mathbb{E}\left[\frac{1}{n_l} \sum_i^{n_l} x_{-;0}^2\right] \right), \quad (3) \\ K_{\perp}^{(l)} &= \frac{1}{4} \left(\mathbb{E}\left[\frac{1}{n_l} \sum_i^{n_l} x_{+;0}^2\right] + \mathbb{E}\left[\frac{1}{n_l} \sum_i^{n_l} x_{-;0}^2\right] - 2\mathbb{E}\left[\frac{1}{n_l} \sum_i^{n_l} x_{+;0} x_{-;0}\right] \right). \end{aligned}$$

As $\delta x \rightarrow 0$, the components $K_{\parallel}^{(l)}$ and $K_{\perp}^{(l)}$ each vanish, while the first term collapses to a degenerate matrix. In Roberts et al. (2022), through a careful eigenvalue expansion one

finds that the two-point activation correlation under this perturbed kernel is given by:

$$\begin{aligned}
 & \langle \sigma(z_\alpha) \sigma(z_\beta) \rangle_{K^{(l)}} \\
 &= \left[\langle \sigma(z_0) \sigma(z_0) \rangle_{K_{00}^{(l)}} \right] \gamma_{\alpha\beta}^{[0]} \\
 &+ \left[\left(\frac{\delta K_{\parallel}^{(l)}}{K_{00}^{(l)}} \right) \langle z_0 \sigma'(z_0) \sigma(z_0) \rangle_{K_{00}^{(l)}} \right] \gamma_{\alpha\beta}^{[1]} \\
 &+ \left[\delta \delta K_{\perp}^{(l)} \langle \sigma'(z_0) \sigma'(z_0) \rangle_{K_{00}^{(l)}} + \left(\frac{\delta K_{\parallel}^{(l)}}{2K_{00}^{(l)}} \right)^2 \langle (z_0^2 - K_{00}^{(l)}) \sigma'(z_0) \sigma'(z_0) \rangle_{K_{00}^{(l)}} \right] \gamma_{\alpha\beta}^{[2]}
 \end{aligned} \tag{4}$$

From that result, one deduces the following recursion relations for the leading terms of $K_{\parallel}^{(l)}$ and $K_{\perp}^{(l)}$:

$$\begin{aligned}
 \delta K_{\parallel}^{(l+1)} &= \frac{C_W}{K} \langle z \sigma'(z) \sigma(z) \rangle_K \delta K_{\parallel}^{(l)}, \\
 \delta \delta K_{\perp}^{(l+1)} &= C_W \langle \sigma'(z) \sigma'(z) \rangle_K \delta \delta K_{\perp}^{(l)} + \frac{C_W}{4K^2} \langle \sigma'(z) \sigma'(z) (z^2 - K) \rangle_K (\delta K_{\parallel}^{(l)})^2.
 \end{aligned} \tag{5}$$

When the perturbation is orthogonal to the data, the second term on the right-hand side of the equation for $\delta \delta K_{\perp}^{(l)}$ vanishes. Consequently, in both the parallel and perpendicular cases the two formulas above reduce to geometric-sequence recursions, and if their common ratios $\frac{C_W}{K} \langle z \sigma'(z) \sigma(z) \rangle_K$ and $C_W \langle \sigma'(z) \sigma'(z) \rangle_K$ both equal one, the volume occupied by the data distribution remains constant as it propagates through the layers.

2.2 Neural Operator

The architecture of the neural operator we consider consists of the following two types of layers: Eq. (6) describes a linear layer that linearly transforms the vector dimension of functional data, and Eq. (7) represents a kernel integration layer performing convolution operations with a kernel function. Eq. (8) expresses the kernel integration layer combined with a non-linear activation function. In general, the kernel function does not need to be translationally invariant; however, in our setting, we focus on the translationally invariant case as expressed in Eq. (7).

$$\left(\mathcal{L}(u)(x) \right)_i := \sum_j W_{ij} u_j(x), \quad i = 1, \dots, n. \tag{6}$$

$$\left(\mathcal{R}(u)(x) \right)_i := \int_{\mathbb{R}^d} k_{ij}(x - x') u_j(x') dx', \quad i = 1, \dots, n. \tag{7}$$

$$\mathfrak{S}(x) := \sigma(\mathcal{R}(u)(x)). \tag{8}$$

Definition 3 By composing the linear layers and kernel-integration layers introduced above, we build the Neural Operator architecture as follows:

$$\begin{aligned}
 \mathcal{Z}^{(1)} &:= \mathcal{L}_{\text{lift}}(u) \\
 \mathcal{Z}^{(l+1)}(u) &:= \mathcal{R}^{(l+1)} \left(\mathfrak{S}^{(l)}(u) \right), \quad l = 1, \dots, L-1, \\
 \mathcal{Y}(u) &:= \mathcal{L}_{\text{proj}} \left(\mathcal{Z}^{(L)}(u) \right).
 \end{aligned} \tag{9}$$

Here, $\mathcal{L}_{\text{lift}}$ and $\mathcal{L}_{\text{proj}}$ are linear layers. $\mathcal{L}_{\text{lift}}$ lifts the input function's pointwise values into a higher-dimensional feature space, $\mathcal{L}_{\text{proj}}$ projects the preactivations—after they have passed through the sequence of kernel-integration layers—back down to the dimensionality of the target function. $\mathcal{R}^{(k)}$ denotes a kernel-integration layer. In the Fourier Neural Operator of Li et al. (2021), each kernel-integration layer is implemented by taking the Fourier transform of its input, multiplying by a learnable tensor, and then applying the inverse Fourier transform. Concretely, one can write:

$$u_i^{(k+1)} \mapsto \sigma \left(\mathcal{F} \left(\sum_j R_{ij}^{(k+1)}(f) \hat{u}_j^{(k)}(f) \right) \right)$$

where $R_{ij}^{(k+1)}(f)$ represents the parameterized complex-valued tensor. We adopt the convention of using \mathcal{F} for the Fourier transform, and \mathcal{F}^{-1} for the inverse transform. As with fully-connected networks, we initialize all parameters so that they follow the following statistical distributions:

$$\begin{aligned} \mathbb{E}[R_{ij}^{(k+1)}(f)] &= 0, \\ \mathbb{E}[\text{Re}(R_{i_1 j_1}^{(k+1)}(f)) \text{Re}(R_{i_2 j_2}^{(k+1)}(f'))] &= \frac{C_{R^{(k+1)}}(f)}{2n_k} \delta_{i_1 i_2} \delta_{j_1 j_2} \delta(f - f'), \\ \mathbb{E}[\text{Im}(R_{i_1 j_1}^{(k+1)}(f)) \text{Im}(R_{i_2 j_2}^{(k+1)}(f'))] &= \frac{C_{R^{(k+1)}}(f)}{2n_k} \delta_{i_1 i_2} \delta_{j_1 j_2} \delta(f - f'), \\ \mathbb{E}[\text{Re}(R_{i_1 j_1}^{(k+1)}(f)) \text{Im}(R_{i_2 j_2}^{(k+1)}(f'))] &= 0. \end{aligned} \tag{10}$$

Therefore, the initialization distribution of the kernel-integration layers can be viewed as white noise, and when implemented in practice via discretization, it matches the setup in Lu et al. (2021). Our neural-operator architecture assumes real-valued functions. To guarantee that multiplying by the parameter tensor $R_{ij}^{(k)}$ and then applying the inverse Fourier transform still yields a real function, we theoretically impose the symmetry on the sampled parameters: $R_{ij}^{(k)}(f) = \overline{R_{ij}^{(k)}}(-f)$. During training the values of $R_{ij}^{(k)}$ evolve, yet the symmetry is preserved in practice because the implementation processes data with a real discrete Fourier transform, which enforces the required conjugate symmetry automatically. For the linear layers, we define their initialization distributions in exactly the same way as in FCN.

3. Effective Field Theory for Neural Operators

Following the effective-field-theory (EFT) framework for neural networks set out in Section 2.1, the functional degrees of freedom u are assumed to follow the Boltzmann type distribution

$$P(u) \propto \exp(-S(u)).$$

where the action $S(u)$ fully determines the statistical weight of each configuration. The expectation value of u at position x is therefore obtained from the path integral

$$\mathbb{E}[u(x)] = \frac{\int u(x) P(u) \mathcal{D}u}{\int P(u) \mathcal{D}u}.$$

Because both differentiation and ordinary integration act linearly on the functional measure, connected correlators furnish a systematic means of computing expectation values that involve products, derivatives, or integrals of multiple fields. In what follows, closed-form expressions for these correlators are derived, and—paralleling the analysis in Section 2—recursive relations are established for the two-point kernel and the four-point vertex. Finally, explicit formulas are provided for the susceptibility of the kernel to perturbations parallel and perpendicular to a chosen reference trajectory in function space, thereby quantifying anisotropic responses to input variations.

3.1 Correlators for Neural Operators

Henceforth, boldface letters indicate vector-valued functions. And notation \hat{u} also means $\mathcal{F}(u)$. Because the explicit evaluation of correlators in layers that include convolution is prohibitively cumbersome, we instead work in Fourier space and compute the correlators of the Fourier-transformed pre-activations. In particular, Eq. (11) gives the two-point correlator of the l -th layer conditioned on the $(l-1)$ -th layer’s outputs \mathbf{u} and \mathbf{v} . We write

$$\left(\mathcal{Z}^{(l)}|_{\mathbf{u}}\right)_i$$

for the i -th component of $\mathcal{Z}^{(l)}|_{\mathbf{u}}$, that is, the i -th pre-activation in layer l when the preceding layer is fixed to the function \mathbf{u} .

$$\begin{aligned} & \mathbb{E}\left[\mathcal{F}\left(\mathcal{Z}^{(l)}|_{\mathbf{u}}\right)_{i_1}(f)\overline{\mathcal{F}\left(\mathcal{Z}^{(l)}|_{\mathbf{v}}\right)_{i_2}(f')}\middle|u, v\right] \\ &= \mathbb{E}\left[\sum_{j_1 j_2} R_{i_1 j_1}^{(l)}(f) \overline{R_{i_2 j_2}^{(l)}(f')} \hat{u}_{j_1}(f) \overline{\hat{v}_{j_2}}(f')\middle|u, v\right] \\ &= \sum_{j_1 j_2} \frac{C_{R^{(l)}}}{n^{(l-1)}} \delta(f - f') \delta_{i_1 i_2} \delta_{j_1 j_2} \hat{u}_{j_1}(f) \overline{\hat{v}_{j_2}}(f') \\ &= \frac{C_{R^{(l)}}}{n^{(l-1)}} \delta(f - f') \delta_{i_1 i_2} \sum_j \hat{u}_j(f) \overline{\hat{v}_j}(f'). \end{aligned} \tag{11}$$

Eq. (12) presents the general form of an arbitrary $2k$ -point connected correlator. Under mild regularity conditions, an inductive estimate shows that the correlator in layer l obeys the scaling $\mathcal{O}(\frac{1}{n^s})$. If the activation function is analytic and vanishes at the origin, the leading contribution to the connected correlator of activations in layer $l-1$ obeys the same bound. In addition, the statistics of the pre-kernel-integration stages match those of a fully connected network, as established in Section 2.1. Hence, when all widths are identical and large, $n = n_l = \dots = n_0, n \gg 1$, the connected correlator in layer l is suppressed to $\mathcal{O}(\frac{1}{n^{k-1}})$. In the infinite-width limit, only the two-point connected correlator carries appreciable statistical weight; the analysis that follows therefore concentrates on the relationship between this kernel and the four-point vertex that governs its fluctuations. For conciseness the derivation in Eq. (12) is given for real-valued functions, but the extension to complex-valued fields is

straightforward.

$$\begin{aligned}
& \mathbb{E} \left[\mathcal{F} \left(\mathcal{Z}^{(l)} \{ \mathbf{u}_1 \} \right)_{i_1} (f_1) \dots \mathcal{F} \left(\mathcal{Z}^{(l)} \{ u_{2k} \} \right)_{i_{2k}} (f_{2k}) \right] \Big|_{\text{conn}} \\
&= \left(\frac{C_{R^{(l)}}}{n^{(l-1)}} \right)^k \delta_{i_1 i_2} \dots \delta_{i_{2k-1} i_{2k}} \delta(f_1 - f_2) \dots \delta(f_{2k-1} - f_{2k}) \\
& \quad \sum_{j_1, \dots, j_{2k}}^{n^{(l-1)}} \delta_{j_1 j_2} \dots \delta_{j_{2k-1} j_{2k}} \left\{ \mathbb{E} \left[\mathcal{F} \left(\mathfrak{S}^{(l-1)} \{ \mathbf{u}_1 \} \right)_{j_1} (f_1) \dots \mathcal{F} \left(\mathfrak{S}^{(l-1)} \{ u_{2k} \} \right)_{j_{2k}} (f_{2k}) \right] \right. \\
& \quad \left. - \sum_{\text{all subdivisions of } (1, \dots, 2k)} \mathbb{E} \left[\mathcal{F} \left(\mathfrak{S}^{(l-1)} \{ u_{\mu_{1,1}} \} \right)_{i_{\mu_{1,1}}} \dots \mathcal{F} \left(\mathfrak{S}^{(l-1)} \{ u_{\mu_{1,t_1}} \} \right)_{i_{\mu_{1,t_1}}} \right] \Big|_{\text{conn}} \dots \right. \\
& \quad \left. \mathbb{E} \left[\mathcal{F} \left(\mathfrak{S}^{(l-1)} \{ u_{\mu_{\nu,1}} \} \right)_{i_{\mu_{\nu,1}}} \dots \mathcal{F} \left(\mathfrak{S}^{(l-1)} \{ u_{\mu_{\nu,t_\nu}} \} \right)_{i_{\mu_{\nu,t_\nu}}} \right] \Big|_{\text{conn}} \right\} \tag{12}
\end{aligned}$$

Although we currently compute all statistical objects for the Fourier transforms of the pre-activation functions, the corresponding quantities in the spatial domain are recovered via Eq. (13). Specifically,

$$\begin{aligned}
& \mathbb{E} \left[\left(\mathcal{Z}^{(l)} |_{\mathbf{u}} (x) \right)_i \overline{\left(\mathcal{Z}^{(l)} |_{\mathbf{v}} (y) \right)_{i'}} \Big| v \right] \\
&= \int_{\mathbb{R}^d} \int_{\mathbb{R}^d} \mathbb{E} \left[\mathcal{F} \left(\mathcal{Z}^{(l)} |_{\mathbf{u}} \right)_i (f) \overline{\mathcal{F} \left(\mathcal{Z}^{(l)} |_{\mathbf{v}} \right)_{i'}} (f') \Big| u \right] e^{ifx} e^{-if'y} df df' \\
&= \frac{C_{R^{(l)}}}{n^{(l-1)}} \delta_{ii'} \mathcal{F}^{-1} \left(\langle \hat{\mathbf{u}}, \hat{\mathbf{v}} \rangle \right) (x - y) \tag{13}
\end{aligned}$$

Now, we consider 2-point correlator for neural operator, since l -th layer parameters and variables upto $(l-1)$ -th layers are independent, the two-point correlator of a neural operator factorizes as Eq. (14).

$$\begin{aligned}
& \mathbb{E} \left[\mathcal{F} \left(\mathcal{Z}^{(l)} \{ \mathbf{u} \} \right)_i (f) \overline{\mathcal{F} \left(\mathcal{Z}^{(l)} \{ \mathbf{v} \} \right)_{i'}} (f') \right] \\
&= \frac{C_{R^{(l)}}}{n^{(l-1)}} \delta_{ii'} \delta(f - f') \mathbb{E} \left[\left(\mathcal{F} \left(\mathfrak{S}^{(l-1)} \{ \mathbf{u} \} \right) (f) \cdot \overline{\mathcal{F} \left(\mathfrak{S}^{(l-1)} \{ \mathbf{v} \} \right) (f')} \right) \right] \tag{14}
\end{aligned}$$

and we define the l -th layer mean metric $\mathcal{G}^{(l)}$ as non-trivial part of (14) as Eq. (15) and stochastic metric $\widetilde{\mathcal{G}}^{(l)}$ as (16) in which expectation is not taken except on last l -th layer:

$$\mathcal{G}^{(l)} \{ \mathbf{u}, \mathbf{v} \} (f, f') := \frac{C_{R^{(l)}}}{n^{(l-1)}} \mathbb{E} \left[\mathcal{F} \left(\mathfrak{S}^{(l-1)} \{ \mathbf{u} \} \right) (f) \cdot \overline{\mathcal{F} \left(\mathfrak{S}^{(l-1)} \{ \mathbf{v} \} \right) (f')} \right] \tag{15}$$

$$\widetilde{\mathcal{G}}^{(l)} \{ \mathbf{u}, \mathbf{v} \} (f, f') := \frac{C_{R^{(l)}}}{n^{(l-1)}} \sum_j \mathcal{F} \left(\mathfrak{S}^{(l-1)} \{ \mathbf{u} \} \right)_j (f) \overline{\mathcal{F} \left(\mathfrak{S}^{(l-1)} \{ \mathbf{v} \} \right)_j (f')} \tag{16}$$

and we define the fluctuation of metric $\Delta \widetilde{\mathcal{G}}^{(l)}$ as follows equation:

$$\begin{aligned}
\Delta \widetilde{\mathcal{G}}^{(l)} \{ \mathbf{u}, \mathbf{v} \} (f, f') &:= \widetilde{\mathcal{G}}^{(l)} (f, f') - \mathcal{G}^{(l)} (f, f') \\
&= \frac{C_{R^{(l)}}}{n^{(l-1)}} \sum_j \left(\mathcal{F} \left(\mathfrak{S}^{(l-1)} \{ \mathbf{u} \} \right)_j (f) \overline{\mathcal{F} \left(\mathfrak{S}^{(l-1)} \{ \mathbf{v} \} \right)_j (f')} - \mathbb{E} \left[\mathcal{F} \left(\mathfrak{S}^{(l-1)} \{ \mathbf{u} \} \right) (f) \cdot \overline{\mathcal{F} \left(\mathfrak{S}^{(l-1)} \{ \mathbf{v} \} \right) (f')} \right] \right) \tag{17}
\end{aligned}$$

Now we define four-point vertex $\mathcal{V}^{(l)}\{(\mathbf{u}_1, \mathbf{u}_2), (\mathbf{u}_3, \mathbf{u}_4)\}$ which is scaled variance of fluctuation $\widetilde{\Delta \mathcal{G}^{(l)}}$. Using this quantity, we can calculate 4-point correlators perturbatively. Eq. (18) shows the expansion of four point vertex which is composed of 4-point connected correlators of $(l-1)$ -th layer activations.

$$\begin{aligned}
& \frac{1}{n^{(l-1)}} \mathcal{V}^{(l)} \{(\mathbf{u}_1, \mathbf{u}_2), (\mathbf{u}_3, \mathbf{u}_4)\} (f_1, f_2, f_3, f_4) := \\
& \mathbb{E} \left[\Delta \widetilde{\mathcal{G}^{(l)}} \{ \mathbf{u}_1, \mathbf{u}_2 \} (f_1, f_2) \Delta \widetilde{\mathcal{G}^{(l)}} \{ \mathbf{u}_3, \mathbf{u}_4 \} (f_3, f_4) \right] \\
& = C_{R^{(l)}}^2 \left(\frac{1}{n^{(l-1)}} \right)^2 \mathbb{E} \left[\sum_{j,k} \left(\mathcal{F} \left(\mathfrak{S}^{(l-1)} \{ \mathbf{u}_1 \} \right)_j (f_1) \mathcal{F} \left(\mathfrak{S}^{(l-1)} \{ \mathbf{u}_2 \} \right)_j (f_2) \right. \right. \\
& \quad \left. \left. - \mathbb{E} \left[\mathcal{F} \left(\mathfrak{S}^{(l-1)} \{ \mathbf{u}_1 \} \right) (f_1) \cdot \mathcal{F} \left(\mathfrak{S}^{(l-1)} \{ \mathbf{u}_2 \} \right) (f_2) \right] \right) \right. \\
& \quad \left(\mathcal{F} \left(\mathfrak{S}^{(l-1)} \{ \mathbf{u}_3 \} \right)_k (f_3) \mathcal{F} \left(\mathfrak{S}^{(l-1)} \{ \mathbf{u}_4 \} \right)_k (f_4) - \mathbb{E} \left[\mathcal{F} \left(\mathfrak{S}^{(l-1)} \{ \mathbf{u}_3 \} \right) (f_3) \cdot \mathcal{F} \left(\mathfrak{S}^{(l-1)} \{ \mathbf{u}_4 \} \right) (f_4) \right] \right) \right] \\
& = C_{R^{(l)}}^2 \left(\frac{1}{n^{(l-1)}} \right)^2 \sum_j \left(\mathbb{E} \left[\mathcal{F} \left(\mathfrak{S}^{(l-1)} \{ \mathbf{u}_1 \} \right)_j (f_1) \mathcal{F} \left(\mathfrak{S}^{(l-1)} \{ \mathbf{u}_2 \} \right)_j (f_2) \right. \right. \\
& \quad \left. \left. \mathcal{F} \left(\mathfrak{S}^{(l-1)} \{ \mathbf{u}_3 \} \right)_j (f_3) \mathcal{F} \left(\mathfrak{S}^{(l-1)} \{ \mathbf{u}_4 \} \right)_j (f_4) \right] - \mathbb{E} \left[\mathcal{F} \left(\mathfrak{S}^{(l-1)} \{ \mathbf{u}_1 \} \right)_j (f_1) \mathcal{F} \left(\mathfrak{S}^{(l-1)} \{ \mathbf{u}_2 \} \right)_j (f_2) \right. \right. \\
& \quad \left. \left. \mathbb{E} \left[\mathcal{F} \left(\mathfrak{S}^{(l-1)} \{ \mathbf{u}_3 \} \right)_j (f_3) \mathcal{F} \left(\mathfrak{S}^{(l-1)} \{ \mathbf{u}_4 \} \right)_j (f_4) \right] \right) \right. \\
& \quad \left. + C_{R^{(l)}}^2 \left(\frac{1}{n^{(l-1)}} \right)^2 \sum_{j \neq k} \left(\mathbb{E} \left[\mathcal{F} \left(\mathfrak{S}^{(l-1)} \{ \mathbf{u}_1 \} \right)_j (f_1) \mathcal{F} \left(\mathfrak{S}^{(l-1)} \{ \mathbf{u}_2 \} \right)_j (f_2) \right. \right. \right. \\
& \quad \left. \left. \mathcal{F} \left(\mathfrak{S}^{(l-1)} \{ \mathbf{u}_3 \} \right)_k (f_3) \mathcal{F} \left(\mathfrak{S}^{(l-1)} \{ \mathbf{u}_4 \} \right)_k (f_4) \right] - \mathbb{E} \left[\mathcal{F} \left(\mathfrak{S}^{(l-1)} \{ \mathbf{u}_1 \} \right)_j (f_1) \mathcal{F} \left(\mathfrak{S}^{(l-1)} \{ \mathbf{u}_2 \} \right)_j (f_2) \right] \right. \\
& \quad \left. \left. \mathbb{E} \left[\mathcal{F} \left(\mathfrak{S}^{(l-1)} \{ \mathbf{u}_3 \} \right)_k (f_3) \mathcal{F} \left(\mathfrak{S}^{(l-1)} \{ \mathbf{u}_4 \} \right)_k (f_4) \right] \right) \right) \tag{18}
\end{aligned}$$

3.2 Running of Couplings

In this subsection, we find the recursive relation of correlation functions which also can be mentioned as running of couplings endowed from the terminology of theoretical physics. First, as the layer widths go to infinity, the metric converges to fixed kernel function we will denote it as $\mathcal{K}^{(l)}$. Then as fluctuation goes to zero, the kernel can be calculated by integrating over Gaussian process which defined by previous layer's kernel:

$$\mathcal{K}^{(l+1)}\{\mathbf{u}, \mathbf{v}\}(f, f') := C^{(l+1)}(f) \langle \mathcal{F}(\mathfrak{S}^{(l)}\{\mathbf{u}\}), \mathcal{F}(\mathfrak{S}^{(l)}\{\mathbf{v}\}) \rangle_{\mathcal{K}^{(l)}}(f, f').$$

Here, notation $\langle A, B \rangle_{\mathcal{K}}(f, f')$ means the expectation value of $A(f)\overline{B(f')}$ where each A and B are Gaussian random fields with kernel \mathcal{K} . We will denote functions $\mathcal{K}\{\mathbf{u}, \mathbf{u}\}$ simply as $\mathcal{K}\{\mathbf{u}\}$ and $\langle A, A \rangle_{\mathcal{K}}$ as $\|A\|_{\mathcal{K}}$. $\mathcal{K}\{\mathbf{u}\}(f)$ will mean the diagonal values $\mathcal{K}\{\mathbf{u}\}(f, f)$. Specifically, the first kernel is defined as in (19) and deeper layer kernels are calculated recursively as in

(20).

$$\mathcal{K}^{(1)}\{\mathbf{u}, \mathbf{v}\}(f, f') := \frac{C_W}{n^{(1)}} \sum_j \hat{u}_j(f) \hat{v}_j(f') \quad (19)$$

$$\begin{aligned} \mathcal{K}^{(l+1)}\{\mathbf{u}\}(f, f') &= \frac{C_{R^{(l+1)}}}{n^{(l+1)}} g(\mathcal{K}^{(l)}\{\mathbf{u}\}(f, f')) \\ g(\mathcal{K}) &:= \langle \mathcal{F}(\mathfrak{S}^{(l)}\{\mathbf{u}\}), \mathcal{F}(\mathfrak{S}^{(l)}\{\mathbf{u}\}) \rangle_{\mathcal{K}^{(l)}}(f, f'). \end{aligned} \quad (20)$$

Next, we describe the recursion for the four-point vertex. In Eq. (18), when all four indices coincide, the distribution reduces to one over a single scalar. Therefore, by computing each statistic similar to as in the nearly Gaussian action expansion of Roberts et al. (2022), we obtain the following expression as in (2):

$$\begin{aligned} & \frac{C_{R^{(l)}}^2}{n^{(l-1)}} \mathcal{V}^{(l)}\{(\mathbf{u}_{\alpha_1}, \mathbf{u}_{\alpha_2}), (\mathbf{u}_{\alpha_3}, \mathbf{u}_{\alpha_4})\} \\ &= \frac{1}{n^{(l)}} \left[\left\langle \mathcal{F}(\mathfrak{S}^{(l-1)})\{\mathbf{u}_{\alpha_1}\} \mathcal{F}(\mathfrak{S}^{(l-1)})\{\mathbf{u}_{\alpha_2}\} \mathcal{F}(\mathfrak{S}^{(l-1)})\{\mathbf{u}_{\alpha_3}\} \mathcal{F}(\mathfrak{S}^{(l-1)})\{\mathbf{u}_{\alpha_4}\} \right\rangle \right] \\ & \quad - \left\langle \mathcal{F}(\mathfrak{S}^{(l-1)})\{\mathbf{u}_{\alpha_1}\} \mathcal{F}(\mathfrak{S}^{(l-1)})\{\mathbf{u}_{\alpha_2}\} \right\rangle \left\langle \mathcal{F}(\mathfrak{S}^{(l-1)})\{\mathbf{u}_{\alpha_3}\} \mathcal{F}(\mathfrak{S}^{(l-1)})\{\mathbf{u}_{\alpha_4}\} \right\rangle \\ & \quad + \frac{1}{4n^{(l-1)}} \sum_{\beta_1, \dots, \beta_4 \in \mathcal{D}} \mathcal{V}_{(l-1)}^{-1}\{(\mathbf{u}_{\beta_1}, \mathbf{u}_{\beta_2}), (\mathbf{u}_{\beta_3}, \mathbf{u}_{\beta_4})\} \\ & \quad \left\langle \left(\mathcal{F}(\mathfrak{S}^{(l-1)})\{\mathbf{u}_{\alpha_1}\} \mathcal{F}(\mathfrak{S}^{(l-1)})\{\mathbf{u}_{\alpha_2}\} \left(\mathcal{F}(\mathcal{Z}^{(l-1)}\{\mathbf{u}_{\beta_1}\}) \mathcal{F}(\mathcal{Z}^{(l-1)}\{\mathbf{u}_{\beta_2}\}) - \mathcal{G}^{(l-1)}\{\mathbf{u}_{\beta_1}, \mathbf{u}_{\beta_2}\} \right) \right) \right\rangle_{\mathcal{G}^{(l-1)}} \\ & \quad \left\langle \left(\mathcal{F}(\mathfrak{S}^{(l-1)})\{\mathbf{u}_{\alpha_3}\} \mathcal{F}(\mathfrak{S}^{(l-1)})\{\mathbf{u}_{\alpha_4}\} \left(\mathcal{F}(\mathcal{Z}^{(l-1)}\{\mathbf{u}_{\beta_1}\}) \mathcal{F}(\mathcal{Z}^{(l-1)}\{\mathbf{u}_{\beta_2}\}) - \mathcal{G}^{(l-1)}\{\mathbf{u}_{\beta_1}, \mathbf{u}_{\beta_2}\} \right) \right) \right\rangle_{\mathcal{G}^{(l-1)}} \\ & \quad + \mathcal{O}\left(\frac{1}{n^2}\right) \end{aligned} \quad (21)$$

As we did for the FCN's criticality condition in Section 2, we now derive the critical condition by writing down recursion relations for perturbations in the data's parallel and perpendicular directions. First, consider two samples that are perturbed in the parallel direction around some reference point. If the output perturbation size at layer l is ϵ , the two samples can be written as $\mathcal{Z}_0(1 + \epsilon)$ and $\mathcal{Z}_0(1 - \epsilon)$. Computing the difference between $\langle \|\mathcal{Z}_0(1 + \epsilon)\|_2^2 \rangle_{\mathcal{K}^{(l)}\{\mathbf{u}_0\}}$ and $\langle \|\mathcal{Z}_0(1 - \epsilon)\|_2^2 \rangle_{\mathcal{K}^{(l)}\{\mathbf{u}_0\}}$ yields $4\mathcal{K}^{(l)}\{\mathbf{u}_0\}\epsilon$, and by performing a Taylor expansion to compute the difference at layer $l + 1$ we obtain the following:

$$\begin{aligned} \|\mathcal{Z}^{(l+1)}|_{\mathcal{Z}_0(1+\epsilon)}\|_{\mathcal{K}^{(l)}\{\mathbf{u}_0\}} &= C_{R^{(l+1)}} \|\mathcal{F}(\mathfrak{S}^{(l)}|_{\mathcal{Z}_0(1+\epsilon)})\|_{\mathcal{K}^{(l)}\{\mathbf{u}_0\}} \\ &= C_{R^{(l+1)}} \|\mathcal{F}(\mathfrak{S}^{(l)}|_{\mathcal{Z}_0}) + \mathcal{F}(\mathcal{Z}_0\mathfrak{S}'^{(l)}|_{\mathcal{Z}_0})\epsilon + \mathcal{O}(\epsilon^2)\|_{\mathcal{K}^{(l)}\{\mathbf{u}_0\}} \\ &\Rightarrow \|\mathcal{Z}^{(l+1)}|_{\mathcal{Z}_0(1+\epsilon)}\|_{\mathcal{K}^{(l)}\{\mathbf{u}_0\}} - \|\mathcal{Z}^{(l+1)}|_{\mathcal{Z}_0(1-\epsilon)}\|_{\mathcal{K}^{(l)}\{\mathbf{u}_0\}} \\ &= 2C_{R^{(l+1)}} \left(\langle \mathcal{F}(\mathcal{Z}_0\mathfrak{S}'^{(l)}|_{\mathcal{Z}_0}), \mathcal{F}(\mathfrak{S}^{(l)}|_{\mathcal{Z}_0})\{\mathbf{u}_0\} \rangle_{\mathcal{K}^{(l)}\{\mathbf{u}_0\}} + \langle \mathcal{F}(\mathfrak{S}^{(l)}|_{\mathcal{Z}_0}), \mathcal{F}(\mathcal{Z}_0\mathfrak{S}'^{(l)}|_{\mathcal{Z}_0}) \rangle_{\mathcal{K}^{(l)}\{\mathbf{u}_0\}} \right) \epsilon. \end{aligned} \quad (22)$$

Therefore, for the difference in variances under parallel perturbations between the l -th and $(l+1)$ -th layers to remain unchanged, the following equation must be satisfied:

$$\begin{aligned}
 \chi_{\parallel}(f, f') &:= \frac{\|\mathcal{Z}^{(l+1)}|_{\mathcal{Z}_0(1+\epsilon)}\|_{\mathcal{K}^{(l)}\{\mathbf{u}_0\}} - \|\mathcal{Z}^{(l+1)}|_{\mathcal{Z}_0(1-\epsilon)}\|_{\mathcal{K}^{(l)}\{\mathbf{u}_0\}}}{\langle \|\mathcal{Z}_0(1+\epsilon)\|_2^2 \rangle_{\mathcal{K}^{(l)}\{\mathbf{u}_0\}} - \langle \|\mathcal{Z}_0(1-\epsilon)\|_2^2 \rangle_{\mathcal{K}^{(l)}\{\mathbf{u}_0\}}} \\
 &= \frac{2C_{R^{(l+1)}} \left(\langle \mathcal{F}(\mathcal{Z}_0 \mathfrak{S}'^{(l)}|_{\mathcal{Z}_0}), \mathcal{F}(\mathfrak{S}^{(l)}|_{\mathcal{Z}_0})\{\mathbf{u}_0\} \rangle_{\mathcal{K}^{(l)}\{\mathbf{u}_0\}} + \langle \mathcal{F}(\mathfrak{S}^{(l)}|_{\mathcal{Z}_0}), \mathcal{F}(\mathcal{Z}_0 \mathfrak{S}'^{(l)}|_{\mathcal{Z}_0}) \rangle_{\mathcal{K}^{(l)}\{\mathbf{u}_0\}} \right) \epsilon}{4\mathcal{K}^{(l)}\{\mathbf{u}_0\}\epsilon} \\
 &= \frac{C_{R^{(l+1)}} \left(\langle \mathcal{F}(\mathcal{Z}_0 \mathfrak{S}'^{(l)}|_{\mathcal{Z}_0}), \mathcal{F}(\mathfrak{S}^{(l)}|_{\mathcal{Z}_0})\{\mathbf{u}_0\} \rangle_{\mathcal{K}^{(l)}\{\mathbf{u}_0\}} + \langle \mathcal{F}(\mathfrak{S}^{(l)}|_{\mathcal{Z}_0}), \mathcal{F}(\mathcal{Z}_0 \mathfrak{S}'^{(l)}|_{\mathcal{Z}_0}) \rangle_{\mathcal{K}^{(l)}\{\mathbf{u}_0\}} \right) (f, f')}{2\mathcal{K}^{(l)}\{\mathbf{u}_0\}(f, f')} \\
 &= 1.
 \end{aligned} \tag{23}$$

Next, we consider perturbations in the perpendicular direction. Strictly speaking, one should analyze the kernel as a 2×2 matrix for the two data points $\mathcal{Z}_+ = \mathcal{Z}_0 + \delta\eta$, $\mathcal{Z}_- = \mathcal{Z}_0 - \delta\eta$. However, if we assume that the perturbation $\delta\eta$ is orthogonal to \mathcal{Z}_0 , all mixed terms related to $\delta\eta \cdot \mathcal{Z}_0$ vanish, and the Gaussian distribution of norms of \mathcal{Z}_0 and perturbations reduce to the form:

$$\mathcal{P} \sim \exp \left(-\frac{\|\mathcal{Z}_0\|(f)^2}{2\mathcal{K}_0(f)} - \frac{\|\delta\eta\|^2(f)}{2\mathcal{K}_\eta} \right) \tag{24}$$

Thus, it is legitimate to express the variance of the difference $\mathfrak{S}^{(1)}\{\mathbf{u}_+\} - \mathfrak{S}^{(1)}\{\mathbf{u}_-\}$ by the simple formula:

$$\begin{aligned}
 &\frac{\|\mathfrak{S}^{(l)}\{\mathbf{u}_+\} - \mathfrak{S}^{(l)}\{\mathbf{u}_-\}\|_{\mathcal{K}^{(l)}}}{4} \\
 &= \frac{\mathcal{K}^{(l+1)}\{\mathbf{u}_+\}(f) + \mathcal{K}^{(l+1)}\{\mathbf{u}_-\}(f) - \mathcal{K}^{(l+1)}\{\mathbf{u}_+, \mathbf{u}_-\}(f) - \mathcal{K}^{(l+1)}\{\mathbf{u}_-, \mathbf{u}_+\}(f)}{4} \\
 &= \frac{\langle \mathcal{F}(\mathfrak{S}^{(l)}\{\mathbf{u}_0\}) + \mathcal{F}(\mathfrak{S}'^{(l)}\{\mathbf{u}_0\}\delta\eta) + \mathcal{O}(\delta\eta^2), \mathcal{F}(\mathfrak{S}^{(l)}\{\mathbf{u}_0\}) + \mathcal{F}(\mathfrak{S}'^{(l)}\{\mathbf{u}_0\}\delta\eta) + \mathcal{O}(\delta\eta^2) \rangle_{\mathcal{K}^{(l)}}}{4} \\
 &+ \frac{\langle \mathcal{F}(\mathfrak{S}^{(l)}\{\mathbf{u}_0\}) - \mathcal{F}(\mathfrak{S}'^{(l)}\{\mathbf{u}_0\}\delta\eta) + \mathcal{O}(\delta\eta^2), \mathcal{F}(\mathfrak{S}^{(l)}\{\mathbf{u}_0\}) - \mathcal{F}(\mathfrak{S}'^{(l)}\{\mathbf{u}_0\}\delta\eta) + \mathcal{O}(\delta\eta^2) \rangle_{\mathcal{K}^{(l)}}}{4} \\
 &- \frac{\langle \mathcal{F}(\mathfrak{S}^{(l)}\{\mathbf{u}_0\}) - \mathcal{F}(\mathfrak{S}'^{(l)}\{\mathbf{u}_0\}\delta\eta) + \mathcal{O}(\delta\eta^2), \mathcal{F}(\mathfrak{S}^{(l)}\{\mathbf{u}_0\}) + \mathcal{F}(\mathfrak{S}'^{(l)}\{\mathbf{u}_0\}\delta\eta) + \mathcal{O}(\delta\eta^2) \rangle_{\mathcal{K}^{(l)}}}{4} \\
 &- \frac{\langle \mathcal{F}(\mathfrak{S}^{(l)}\{\mathbf{u}_0\}) + \mathcal{F}(\mathfrak{S}'^{(l)}\{\mathbf{u}_0\}\delta\eta) + \mathcal{O}(\delta\eta^2), \mathcal{F}(\mathfrak{S}^{(l)}\{\mathbf{u}_0\}) - \mathcal{F}(\mathfrak{S}'^{(l)}\{\mathbf{u}_0\}\delta\eta) + \mathcal{O}(\delta\eta^2) \rangle_{\mathcal{K}^{(l)}}}{4} \\
 &= \left\| \mathcal{F}(\mathfrak{S}'^{(l)}\{\mathbf{u}_0\}) * \mathbb{E}[\delta\eta] \right\|_{\mathcal{K}^{(l)}} + \mathcal{O}(|\delta\eta|^3).
 \end{aligned} \tag{25}$$

Since the variance of $\mathbf{u}_+ - \mathbf{u}_-$ at the l -th layer is $4\mathbb{E}[(\delta\eta)^2]$ and the variance of the preactivation at the $l+1$ -th layer is derived in Eq. (25) the variance of the difference between the two data points will remain constant across layers only if the corresponding

condition is satisfied:

$$\begin{aligned}\chi_{\perp}(f, f') &:= \frac{\|\mathcal{Z}^{(l+1)}|_{\mathcal{Z}_0+\delta\eta} - \mathcal{Z}^{(l+1)}|_{\mathcal{Z}_0-\delta\eta}\|_{\mathcal{K}^{(l)}\{u_0\}, \mathcal{K}_{\eta}\{\delta\eta\}}}{\|(\mathcal{Z}_0 + \delta\eta) - (\mathcal{Z}_0 - \delta\eta)\|_{\mathcal{K}_{\eta}}} \\ &= \delta(f - f') C_{R^{(l+1)}} \frac{\left\| \mathcal{F}(\mathfrak{S}'^{(l)}\{u_0\}) * \mathbb{E}[\delta\eta] \right\|_{\mathcal{K}^{(l)}}}{\mathbb{E}[\delta\eta(f)\delta\eta(f')]} = 1.\end{aligned}\quad (26)$$

Note that parallel and perpendicular susceptibilities are defined at different perturbative orders. Because the perturbation is orthogonal to the input in the perpendicular case, the leading non-vanishing contribution appears at second order in the small perturbation $\delta\eta$. By contrast, a perturbation parallel to the input produces a non-zero contribution already at first order along parameter ϵ . Each susceptibility is therefore defined in terms of the fluctuation that arises at its respective lowest non-trivial order. Accordingly, for local fluctuations to remain stable under perturbations perpendicular to the reference trajectory, the following condition must be satisfied:

$$\delta(f - f') C_{R^{(l+1)}} \left(\left\| \mathcal{F}(\mathfrak{S}'^{(l)}\{u_0\}) * \mathbb{E}[\delta\eta] \right\|_{\mathcal{K}^{(l)}} \right) (f, f') = \mathbb{E}[\delta\eta(f)\delta\eta(f')]. \quad (27)$$

Imposing that relation Eq. (27) exactly would make $\|\mathcal{F}(\mathfrak{S}'^{(l)}\{u_0\})\|_{\mathcal{K}^{(l)}\{u_0\}}$ behave like a Dirac delta, which is too restrictive for most practical networks. Instead, we adopt a softer requirement: the integrated (layer-wise) sum of the kernel remains constant across layers, so the overall spectral energy is preserved while still allowing a non-trivial, spatially extended kernel shape.

$$\begin{aligned}\int \delta(f - f') C_{R^{(l+1)}} \|\mathcal{F}(\mathfrak{S}'^{(l)}\{u_0\})\|_{\mathcal{K}^{(l)}\{u_0\}} * \mathbb{E}[(\delta\eta)^2] df df' &= \int \mathbb{E}[(\delta\eta)^2] df df' \\ \Rightarrow \int \delta(f - f') C_{R^{(l+1)}} \|\mathcal{F}(\mathfrak{S}'^{(l)}\{u_0\})\|_{\mathcal{K}^{(l)}\{u_0\}}(f, f') df df' &= 1 \\ \Rightarrow \int C_{R^{(l+1)}}(f) \|\mathcal{F}(\mathfrak{S}'^{(l)}\{u_0\})\|_{\mathcal{K}^{(l)}\{u_0\}}(f) df &= 1.\end{aligned}\quad (28)$$

For convenience we introduce the reduced perpendicular susceptibility

$$\tilde{\chi}_{\perp}(f, f') := \|\mathcal{F}(\mathfrak{S}'^{(l)}\{u_0\})\|_{\mathcal{K}^{(l)}\{u_0\}}$$

With this notation, the analysis of correlators and their recursion relations yields three depth-wise critical conditions:

$$\begin{aligned}\chi_{\parallel} &\equiv 1, \quad \text{local condition} \\ \int C(f) \tilde{\chi}_{\perp}(f) df &\equiv 1 \quad \text{global condition.}\end{aligned}\quad (29)$$

4. Special Cases

In this section we put the general framework of Section 3 to work by carrying out the calculation in three representative settings—(i) analytic activations, (ii) scale-invariant architectures, and (iii) networks equipped with residual connections. To handle the non-linearity introduced by an analytic activation in Fourier space, we first state the following lemma.

Lemma 1 Let $\sigma : \mathbb{R} \rightarrow \mathbb{R}$ be an analytic function passing through the origin and $g \in L^1$ such that $\sigma(g) \in L^1$ then,

$$\text{For } \sigma(x) = \sum_{n=1}^{\infty} \frac{\sigma_n}{n!} x^n,$$

$$\mathcal{F}(\sigma(g))(f) = \sum_{n=1}^{\infty} \frac{\sigma_n}{n!} \hat{g}^{*n}(f).$$

where \hat{g}^{*n} means n -times self-convolution of \hat{g} .

Proof. $\sum_{k=1}^n \frac{\sigma_k}{k!} g(x)^k e^{-ifx}$ converges pointwise to $\sigma(g(x))e^{-ifx}$ and

$$| \sum_{k=1}^n \frac{\sigma_k}{k!} g(x)^k e^{-ifx} | \leq \sum_{k=1}^{\infty} \frac{\sigma_k}{k!} |g(x)|^k = \sigma(g(x)). \quad (30)$$

So, by dominated convergence theorem we have following equation:

$$\begin{aligned} \int \sigma(g(x))e^{-ifx} dx &= \sum_{k=1}^{\infty} \int \frac{\sigma_k}{k!} g^k(x) e^{-ifx} dx \\ &= \sum_{k=1}^{\infty} \frac{\sigma_k}{k!} \mathcal{F}(g^k) = \sum_{n=1}^{\infty} \frac{\sigma_n}{n!} \hat{g}^{*n}. \end{aligned} \quad (31)$$

□

4.1 Analytic Activations

First, we consider the case where the activation is an analytic function so that we can expand it and kernels perturbatively. Suppose the activation passes through the origin then it can be written as Eq. (32).

$$\sigma(x) := \sum_{n=1}^{\infty} \frac{\sigma_n}{n!} x^n \quad (32)$$

Then, the kernel can be written as follows:

$$\begin{aligned} \mathcal{K}^{(l+1)}\{\mathbf{u}\}(f) &= C_{R^{(l+1)}}(f) \int \left\| \mathcal{F}(\sigma(k^{(l)} * u)) \right\|^2(f) e^{-\int \frac{1}{2\mathcal{K}^{(l)}\{\mathbf{u}\}(f)} \hat{u}(f)^2 df} \mathcal{D}u \\ &= \int \sum_i \frac{1}{n^{(l)}} \left\| \sigma_1 R_{ij}^{(l)}(f) \hat{u}_j(f) + \frac{\sigma_2}{2!} \left((R_{ij}^{(l)} \hat{u}_j) * (R_{ij'}^{(l)} \hat{u}_{j'}) \right)(f) + \dots \right\|^2 e^{-\int \frac{1}{2\mathcal{K}^{(l)}\{\mathbf{u}\}(f)} \hat{u}(f)^2 df} \mathcal{D}u \end{aligned}$$

When the network output is expanded analytically and its Fourier transform is taken, the result can be written as a sum of terms in which a Gaussian random field is composed with itself multiple times. Evaluating those terms requires Lemma 2. The lemma is stated for complex, scalar-valued fields, but the vector-valued case follows immediately: simply apply the lemma component-wise, using the distributive property to handle each vector entry separately.

Lemma 2 Suppose independent, mean-zero Gaussian random fields $\{R(f)\}_{f \in \mathbb{R}}, \{U(f)\}_{f \in \mathbb{R}}$ have following 2-point correlators:

$$\begin{aligned}\mathbb{E}[R(f)\overline{R(f')}] &= \delta(f - f')C(f), \\ \mathbb{E}[\text{Re}(R(f))\text{Im}(R(f'))] &= 0, \\ \mathbb{E}[U(f)U(f')] &= K(f, f').\end{aligned}$$

then we have following relations:

$$\begin{aligned}\mathbb{E}[(RU)^{*n}(f)(\overline{RU})^{*m}(f')] \\ = \delta_{n,m}(n!)^2\delta(f - f')H^{*n}(f').\end{aligned}$$

where $H(f) = C(f)K(f, f)$.

Proof.

$$\begin{aligned}\mathbb{E}[(RU)^{*n}(f)(\overline{RU})^{*m}(f')] \\ = \mathbb{E}\left[\int \delta(f - \sum_{k=1}^n f^{(k)}) \prod_{k=1}^n (RU)(f^{(k)}) df^{(k)} \int \delta(f' - \sum_{k=1}^m f'^{(k)}) \prod_{k=1}^m (\overline{RU})(f'^{(k)}) df'^{(m)}\right] \\ = \int \delta(f - \sum_{k=1}^n f^{(k)}) \delta(f' - \sum_{k=1}^m f'^{(k)}) \mathbb{E}\left[\prod_{k=1}^n \prod_{l=1}^m R(f^{(k)}) \overline{R}(f^{(l)})\right] \mathbb{E}\left[\prod_{k=1}^n \prod_{l=1}^m U(f^{(k)}) \overline{U}(f^{(l)})\right] \prod_{k=1}^n \prod_{l=1}^m df^{(k)} df'^{(l)}\end{aligned}\tag{33}$$

if $n \neq m$, the expectation of $\prod_{l=1}^m R(f^{(k)}) \overline{R}(f^{(l)})$ is zero since the wick contraction of each term contains expectation of R^2 or \overline{R}^2 . So assuming $n = m$ then,

$$\begin{aligned}\mathbb{E}[(RU)^{*n}(f)(\overline{RU})^{*m}(f')] \\ = \delta_{n,m} \int \delta(f - \sum_{k=1}^n f^{(k)}) \delta(f' - \sum_{k=1}^n f'^{(k)}) \mathbb{E}\left[\prod_{k=1}^n \prod_{l=1}^n R(f^{(k)}) \overline{R}(f'^{(l)})\right] \mathbb{E}\left[\prod_{k=1}^n \prod_{l=1}^n U(f^{(k)}) \overline{U}(f'^{(l)})\right] \prod_{k=1}^n \prod_{l=1}^n df^{(k)} df'^{(l)} \\ = \delta_{n,m} \int \delta(f - \sum_{k=1}^n f^{(k)}) \delta(f' - \sum_{k=1}^n f'^{(k)}) (n!)^2 \left(\prod_{k=1}^n \delta(f^{(k)} - f'^{(k)}) C(f^{(k)})\right) \left(\prod_{k=1}^n K(f^{(k)}, f'^{(k)})\right) \prod_{k=1}^n df^{(k)} df'^{(k)} \\ = \delta_{n,m} (n!)^2 \int \delta(f - \sum_{k=1}^n f^{(k)}) \delta(f' - \sum_{k=1}^n f'^{(k)}) \left(\prod_{k=1}^n \delta(f^{(k)} - f'^{(k)}) C(f^{(k)})\right) \left(\prod_{k=1}^n K(f^{(k)}, f'^{(k)})\right) \prod_{k=1}^n df^{(k)} df'^{(k)} \\ = \delta_{n,m} (n!)^2 \int \delta(f - \sum_{k=1}^n f^{(k)}) \delta(f' - \sum_{k=1}^n f^{(k)}) \left(\prod_{k=1}^n H(f^{(k)})\right) \prod_{k=1}^n df^{(k)} \\ = \delta_{n,m} (n!)^2 \delta(f - f') H^{*n}(f').\end{aligned}\tag{34}$$

□

Using Lemma 2, we can now express the kernel of the next layer in terms of the current layer's kernel through the following expansion:

$$\begin{aligned}
 \mathcal{K}^{(l+1)}(f, f') &= \sum_i \frac{C_{R^{(l+1)}}(f)}{n^{(l+1)}} \left\| \left(\sigma_1 R_{ij}^{(l)}(f) \hat{u}_j(f) + \frac{\sigma_2}{2!} \left((R_{ij}^{(l)} \hat{u}_j) * (R_{ij'}^{(l)} \hat{u}_{j'}) \right)(f) + \dots \right) \right\|_{\mathcal{K}^{(l)}} \\
 &= C_{R^{(l+1)}}(f) \sum_i \frac{1}{n^{(l)}} \sum_{k=1}^{\infty} \frac{\sigma_k^2}{(k!)^2} \left\| (R_{ij}^{(l)}(f) \hat{u}_j(f))^{*k} \right\|_{\mathcal{K}^{(l)}} \\
 &= \delta(f - f') C_{R^{(l+1)}}(f) \sum_{k=1}^{\infty} \frac{\sigma_k^2}{(n^{(l)})^{k-1}} \sum_{n_{k,1} + \dots + n_{k,l} = k} \frac{(n_{k,1})! \dots (n_{k,l})!}{k!} (\mathcal{H}^{(l)})^{*n_{k,1}} \dots (\mathcal{H}^{(l)})^{*n_{k,l}}(f)
 \end{aligned}$$

We will frequently use the notation $\mathcal{H}^{(l)}(f) := \mathcal{K}^{(l)}(f)C(f)$; in the discrete case, $\mathcal{H}^{(l)}(n) := \mathcal{K}^{(l)}(n)C(n)$. In the second line, every term that cannot be paired with its complex conjugate drops out by Lemma 2. Combinatorially, at order k , the number of surviving monomials associated with a multiplicity vector $(n_{k,1}, \dots, n_{k,l})$ is $\frac{k!}{n_{k,1}! \dots n_{k,l}!}$. Applying Lemma 2 once more, each pair of identical factors contributes an additional factor $(n_{k,j}!)^2$. Collecting these factors for all indices produces the coefficients $\frac{(n_{k,1})! \dots (n_{k,l})!}{k!}$ which yields the expression shown in the third line. And for parallel susceptibility, we get following:

$$\begin{aligned}
 \chi_{\parallel}(f, f') &= \\
 &= \frac{C_{R^{(l+1)}} \left(\langle \mathcal{F}(\mathcal{Z}_0 \mathfrak{S}'^{(l)}|_{\mathcal{Z}_0}), \mathcal{F}(\mathfrak{S}^{(l)}|_{\mathcal{Z}_0}) \{ \mathbf{u}_0 \} \rangle_{\mathcal{K}^{(l)} \{ u_0 \}} + \langle \mathcal{F}(\mathfrak{S}^{(l)}|_{\mathcal{Z}_0}), \mathcal{F}(\mathcal{Z}_0 \mathfrak{S}'^{(l)}|_{\mathcal{Z}_0}) \rangle_{\mathcal{K}^{(l)} \{ u_0 \}} \right)}{2\mathcal{K}^{(l)} \{ \mathbf{u}_0 \}} \\
 &= C_{R^{(l+1)}} \frac{\sum_i \frac{1}{n^{(l)}} \left\langle \sum_{k=1}^{\infty} \frac{\sigma_k}{(k-1)!} \left(R_{ij}^{(l)}(f) \hat{u}_i(f) \right)^{*k}, \sum_{k=1}^{\infty} \frac{\sigma_k}{(k)!} \left(R_{ij}^{(l)}(f) \hat{u}_i(f) \right)^{*k} \right\rangle_{\mathcal{K}^{(l)}}}{\mathcal{K}^{(l)} \{ \mathbf{u}_0 \}} \\
 &= C_{R^{(l+1)}} \sum_i \frac{1}{n^{(l)}} \sum_{k=1}^{\infty} \frac{\sigma_k^2}{(k-1)! k!} \frac{\langle (R_{ij}^{(l)}(f) \hat{u}_j(f))^{*k}, (R_{ij}^{(l)}(f) \hat{u}_j(f))^{*k} \rangle_{\mathcal{K}^{(l)}}}{\mathcal{K}^{(l)} \{ \mathbf{u}_0 \}} \\
 &= \delta(f - f') C_{R^{(l+1)}} \sum_{k=1}^{\infty} \frac{\sigma_k^2}{(n^{(l)})^{k-1}} \sum_{n_{k,1} + \dots + n_{k,l} = k} \frac{(n_{k,1})! \dots (n_{k,l})!}{(k-1)!} \frac{(\mathcal{H}^{(l)})^{*n_{k,1}} \dots (\mathcal{H}^{(l)})^{*n_{k,l}}(f)}{\mathcal{K}^{(l)} \{ \mathbf{u}_0 \}(f)}.
 \end{aligned}$$

and for perpendicular susceptibility, we get following:

$$\begin{aligned}
 \tilde{\chi}_{\perp}(f, f') &= \|\mathcal{F}(\mathfrak{S}'^{(l)} \{ \mathbf{u}_0 \})\|_{\mathcal{K}^{(l)} \{ u_0 \}} \\
 &= \sum_i \frac{1}{n^{(l)}} \|\sigma_1 + \sigma_2 R_{ij}^{(l)}(f) \hat{u}_j(f) + \frac{\sigma_3}{2!} \left((R_{ij}^{(l)} \hat{u}_j) * (R_{ij'}^{(l)} \hat{u}_{j'}) \right)(f) + \dots\|_{\mathcal{K}^{(l)} \{ u_0 \}} \\
 &= \delta(f - f') \sum_{k=1}^{\infty} \frac{\sigma_k^2}{(n^{(l)})^{k-1}} \sum_{n_{k,1} + \dots + n_{k,l} = k-1} \frac{(n_{k,1})! \dots (n_{k,l})!}{(k-1)!} (\mathcal{H}^{(l)})^{*n_{k,1}} \dots (\mathcal{H}^{(l)})^{*n_{k,l}}(f).
 \end{aligned}$$

In summary, we have following equations for kernel recursion and susceptibilities.

Theorem 1 With the analytic, origin-passing activation specified in Eq. (32) and a Fourier Neural Operator defined by Eq. (9) under the initialization ensemble (10), the kernel and the susceptibilities are given by the following recursion relations:

$$\begin{aligned}\mathcal{K}^{(l+1)}(f, f') &= \delta(f - f') C_{R^{(l+1)}}(f) \sum_{k=1}^{\infty} \frac{\sigma_k^2}{(n^{(l)})^{k-1}} \sum_{n_{k,1}+\dots+n_{k,l}=k} \frac{(n_{k,1})! \dots (n_{k,l})!}{k!} (\mathcal{H}^{(l)})^{*n_{k,1}} \dots (\mathcal{H}^{(l)})^{*n_{k,l}}(f) \\ \chi_{\parallel}(f, f') &= \delta(f - f') C_{R^{(l+1)}}(f) \sum_{k=1}^{\infty} \frac{\sigma_k^2}{(n^{(l)})^{k-1}} \sum_{n_{k,1}+\dots+n_{k,l}=k} \frac{(n_{k,1})! \dots (n_{k,l})!}{(k-1)!} \frac{(\mathcal{H}^{(l)})^{*n_{k,1}} \dots (\mathcal{H}^{(l)})^{*n_{k,l}}(f)}{\mathcal{K}^{(l)}\{\mathbf{u}_0\}(f)}, \\ \tilde{\chi}_{\perp}(f, f') &= \sum_{k=1}^{\infty} \frac{\sigma_k^2}{(n^{(l)})^{k-1}} \sum_{n_{k,1}+\dots+n_{k,l}=k-1} \frac{(n_{k,1})! \dots (n_{k,l})!}{(k-1)!} (\mathcal{H}^{(l)})^{*n_{k,1}} \dots (\mathcal{H}^{(l)})^{*n_{k,l}}(f).\end{aligned}$$

4.2 Scale-Invariant Activations

The scale-invariant class of activations is defined as follows:

$$\sigma(z) := \begin{cases} \alpha z & \text{for } z \geq 0 \\ \beta z & \text{for } z < 0. \end{cases} \quad (35)$$

Since the sequence of functions $\sigma_n(x) = \frac{x}{2}(1 + \text{erf}(nx))$ converges to $\max(x, 0)$, we have the following approximation:

Lemma 3 Let $\text{ReLU}(x) := \max(x, 0)$ then we have following convergent function sequence.

$$\text{ReLU}(x) \simeq \sigma_n(x) = \frac{1}{2}x + \frac{n}{\sqrt{\pi}}x^2 - \frac{n^3}{3\sqrt{\pi}}x^4 + \dots$$

And to approximate the correlation of ReLU via σ_n 's, we need following lemma:

Lemma 4 Suppose g_n converges pointwise to g and $h \in L^1 \cap L^\infty$, satisfying the following conditions:

- $g_n(x) \leq C|x|$ for some constant $C > 0$.

then we have following:

$$\mathcal{F}(g_n \circ h) \rightarrow \mathcal{F}(g \circ h) \quad (\text{uniformly})$$

Proof.

$$|g_n \circ h(x)| \leq C|h(x)| \quad (36)$$

So, $\{g_n(h)\}$ is dominated by f . By dominated convergence theorem we get following:

$$\lim_{n \rightarrow \infty} \int |g_n \circ h(x) - g \circ h(x)| dx = 0 \quad (37)$$

then, from following inequality we get the uniform convergence of $g_n \circ h$ to $g(h)$:

$$|\mathcal{F}(g_n \circ h) - \mathcal{F}(g \circ h)| \leq \int |(g_n \circ h - g \circ h)e^{-ifx}| dx = \int |g_n \circ h - g \circ h| dx = \|g_n \circ h - g \circ h\|_{L^1}. \quad (38)$$

□

Lemma 5 Suppose mean zero Gaussian random fields $\{R(f)\}_{f \in \mathbb{R}}, \{U(f)\}_{f \in \mathbb{R}}$ have following 2-point correlators:

$$\begin{aligned}\mathbb{E}[R(f)R(f')] &= \delta(f - f')C(f), \\ \mathbb{E}[U(f)U(f')] &= K(f, f').\end{aligned}$$

then we have following relations:

$$\mathbb{E}\left[\left\|\text{ReLU}\left(\int UdR\right)\right\|^2\right] = \frac{1}{2} \int C(f)K(f)df. \quad (39)$$

Proof. By Ito isometry we have following identity:

$$\mathbb{E}\left[\left\|\left(\int UdR\right)\right\|^2\right] = \int C(f)K(f)df. \quad (40)$$

And since the expectation of $\int UdR$ is zero, only half of samples affects to the expectation of first equation. So by halving Eq. (40), we get the result. \square

To compute the covariance value of absolute of random variables, we need following lemmas from Heydenreich and Hofstad (2009), Vleck (1943).

Lemma 6 For two Gaussian random variables X, Y with means zero and correlation ρ , the expectation of $|X||Y|$ is formulated as follows:

$$\begin{aligned}\mathbb{E}[|X||Y|] &= \frac{2}{\pi}(\sqrt{1 - \rho^2} + \rho \arcsin \rho), \\ \mathbb{E}[1_{\{X>0\}}1_{\{Y>0\}}] &= \frac{1}{4} + \frac{1}{2\pi} \arcsin \rho.\end{aligned} \quad (41)$$

Lemma 7 Suppose mean zero complex-valued Gaussian random fields $\{R(f)\}_{f \in \mathbb{R}}, \{U(f)\}_{f \in \mathbb{R}}$ have following 2-point correlators:

$$\begin{aligned}\mathbb{E}[R(f)\bar{R}(f')] &= \delta(f - f')C(f), \\ \mathbb{E}[U(f)] &= m(f), \\ \mathbb{E}[U(f)\bar{U}(f')] &= K(f, f').\end{aligned}$$

let define random fields $I(x), H(x)$ as follows:

$$\begin{aligned}I(x) &:= \text{ReLU}\left(\int R(f)U(f)e^{ifx}df\right), \\ h(x) &:= 1_{\{\int R(f)U(f)e^{ifx}df > 0\}}.\end{aligned}$$

then the mean and 2-point correlators are calculated as follows:

$$\begin{aligned}\mathbb{E}[I(x)] &= \frac{1}{\sqrt{2\pi}}V^{\frac{1}{2}} \quad \text{for all } x \in \mathbb{R}, \\ \mathbb{E}[H(x)] &= \frac{1}{2} \quad \text{for all } x \in \mathbb{R}, \\ \mathbb{E}[I(x)\bar{I}(x')] &= \frac{V}{4\pi}(2\sqrt{1 - \rho^2} + \rho(\pi + 2 \arcsin \rho)), \\ \mathbb{E}[h(x)\bar{h}(x')] &= \frac{1}{4} + \frac{1}{2\pi} \arcsin \rho, \\ \mathbb{E}[\bar{R}(f')\bar{U}(f')\mathcal{F}(I(x))] &= \frac{1}{2}\delta(f - f')K(f, f')C(f)\end{aligned}$$

where

$$V = \int C(f)K(f, f)df,$$

$$V\rho(x, x') = \int C(f)K(f, f)\cos(f(x - x'))df.$$

Proof. Firstly, since for fixed $x \in \mathbb{R}$, $\int R(f)U(f)e^{ifx}df$ is an mean-zero Gaussian distribution with variance $V := \int C(f)K(f, f)df$. The mean of $I(x)$ which can be seen as a mean over Truncated Gaussian distribution is as follows:

$$\mathbb{E}[I(x)] = \sqrt{\frac{V}{2\pi}}. \quad (42)$$

and we can decompose ReLU activation into sum of $\frac{x}{2}$ and $\frac{|x|}{2}$. So, we get following:

$$\begin{aligned} & \mathbb{E}[I(x)\bar{I}(x')] \\ &= \mathbb{E}\left[\frac{\left(\int R(f)U(f)e^{ifx}df + \left|\int R(f)U(f)e^{ifx}df\right|\right)\left(\int \bar{R}(f)\bar{U}(f)e^{-ifx'}df + \left|\int \bar{R}(f)\bar{U}(f)e^{-ifx'}df\right|\right)}{4}\right] \\ &= \frac{1}{4}\left(\mathcal{F}_x^{-1}\mathcal{F}_{x'}^{-1}\left(\mathbb{E}[R(f)\bar{R}(f')]\mathbb{E}[U(f)U(f')]\right) + \mathbb{E}[R(f)\bar{R}(f')U(f)\bar{U}(f')1_{\int R(f)U(f)e^{ifx}df > 0}] \right. \\ &\quad \left. + \mathbb{E}[R(f)\bar{R}(f')U(f)\bar{U}(f')1_{\int R(f)U(f)e^{ifx'}df > 0}]\right) + \mathbb{E}\left[\left|\int R(f)U(f)e^{ifx}df\right|\left|\int \bar{R}(f)\bar{U}(f)e^{-ifx'}df\right|\right] \\ &= \frac{1}{4}\left(\mathcal{F}_x^{-1}\mathcal{F}_{x'}^{-1}\left(\delta(f - f')C(f)K(f, f')\right) + V\frac{2}{\pi}\left(\sqrt{1 - \rho^2} + \rho \arcsin \rho\right)\right) \\ &= \frac{V}{4\pi}(2\sqrt{1 - \rho^2} + \rho(\pi + 2 \arcsin \rho)). \end{aligned} \quad (43)$$

It is clear that $\mathbb{E}[H(x)] = \frac{1}{2}$ and the result for $\mathbb{E}[H(x)\bar{H}(x')]$ follows directly from the second equation of Lemma 6. Finally for the last equation, we have following equation:

$$\begin{aligned} & \mathbb{E}[\bar{R}(f')\bar{U}(f')\mathcal{F}I(x)] \\ &= \mathcal{F}(\mathbb{E}[\bar{R}(f')\bar{U}(f')I(x)]). \end{aligned}$$

since $\int R(f)U(f)e^{ifx}df$ is mean-zero the second line of following equations holds,

$$\begin{aligned} \mathcal{F}(\mathbb{E}[\bar{R}(f')\bar{U}(f')I(x)]) &= \mathcal{F}(\mathbb{E}[\int \bar{R}(f')R(f)\bar{U}(f')U(f)e^{ifx}1_{I(x)>0}]) \\ &= \mathcal{F}\frac{1}{2}\mathbb{E}[\mathcal{F}^{-1}(\bar{R}(f')R(f)\bar{U}(f')U(f))] \\ &= \frac{1}{2}\mathcal{F}\mathcal{F}^{-1}\mathbb{E}[\bar{R}(f')R(f)\bar{U}(f')U(f)] \\ &= \frac{1}{2}\delta(f - f')K(f, f')C(f). \end{aligned}$$

□

Now, consider the fourier transform $\mathcal{F}(\mathfrak{S}^{(l)}\{\mathbf{u}\})$ in the case of scale-invariant activation. we have

$$\mathcal{F}(\mathfrak{S}^{(l)}\{\mathbf{u}\}) = (\alpha - \beta) \int \text{ReLU}(\int R_{ij}^{(l)} \hat{u}_j e^{ifx} df) e^{-ifx} dx + \beta(R_{ij}^{(l)} \hat{u}_j).$$

then

$$\begin{aligned} & \mathbb{E} \left[\mathcal{F}(\mathfrak{S}^{(l)}\{\mathbf{u}\}) \overline{\mathcal{F}(\mathfrak{S}^{(l)}\{\mathbf{u}\})} \right] (f, f') \\ & \Rightarrow \mathbb{E} \left[(\alpha - \beta)^2 \int \text{ReLU}(\int R_{ij}^{(l)} \hat{u}_j e^{ifx} df) e^{-ifx} dx \int \overline{\text{ReLU}(\int R_{ij}^{(l)} \hat{u}_j e^{ifx} df) e^{if'x}} dx \right. \\ & \quad + (\alpha - \beta) \beta \overline{(R_{ij}^{(l)} \hat{u}_j)} \int \text{ReLU}(\int R_{ij}^{(l)} \hat{u}_j e^{ifx} df) e^{-ifx} dx \\ & \quad + (\alpha - \beta) \beta (R_{ij}^{(l)} \hat{u}_j) \int \overline{\text{ReLU}(\int R_{ij}^{(l)} \hat{u}_j e^{ifx} df) e^{-if'x}} dx' + \beta^2 (R_{ij}^{(l)} \hat{u}_j) \overline{(R_{ij}^{(l)} \hat{u}_j)} \left. \right] \\ & = (\alpha - \beta)^2 \int \int \left(\frac{V}{4\pi} (2\sqrt{1 - \rho^2} + \rho(\pi + 2 \arcsin \rho)) \right) e^{-ifx + if'x'} dx dx' \\ & \quad (\alpha - \beta) \beta \delta(f - f') C(f) \mathcal{K}(f, f') + \beta^2 \delta(f - f') C(f) \mathcal{K}(f, f'). \end{aligned} \tag{44}$$

And from the fact that $\int (f * g)(x) dx = (\int f(x) dx)(\int g(x) dx)$ we can calculate the total integration of kernel over the 2-point frequency domain by transforming the convoluted terms into geometric terms:

$$\begin{aligned} & \int \int \mathbb{E} \left[\mathcal{F}(\mathfrak{S}^{(l)}\{\mathbf{u}\}) \overline{\mathcal{F}(\mathfrak{S}^{(l)}\{\mathbf{u}\})} \right] (f, f') df df' \\ & \simeq \mathbb{E} \left[(\alpha - \beta)^2 \sigma_n \left(\int \hat{u}_j R_{ij}^{(l)}(df) \right) \overline{\sigma_n \left(\int \hat{u}_j R_{ij}^{(l)}(df') \right)} + (\alpha - \beta) \beta \int \overline{\hat{u}_j R_{ij}^{(l)}(df')} \sigma_n \left(\int \hat{u}_j R_{ij}^{(l)}(df) \right) \right. \\ & \quad \left. + (\alpha - \beta) \beta \int \hat{u}_j R_{ij}^{(l)}(df) \overline{\sigma_n \left(\int \hat{u}_j R_{ij}^{(l)}(df') \right)} + \beta^2 \int R_{ij}^{(l)}(f) \overline{R_{ij'}^{(l)}(f')} \hat{u}_j(f) \hat{u}_{j'}(f') df df' \right] \\ & \Rightarrow \int \langle \mathcal{F} \mathfrak{S}^{(l)}\{\mathbf{u}_0\}, \mathcal{F} \mathfrak{S}^{(l)}\{\mathbf{u}_0\} \rangle_{\mathcal{K}^{(l)}\{\mathbf{u}_0, \mathbf{u}_0\}} (f, f') df df' \\ & = \frac{\alpha^2 + \beta^2}{2} \int \mathcal{H}^{(l)}(f) df. \end{aligned}$$

If you see Eq. (44), if α is not zero, the first term survives which mixing all the components in positional domain. Then this term makes the kernel not to vanish over the truncated frequencies. And now we consider the parallel susceptibility. For that we first consider following term:

$$\begin{aligned} & \langle \mathcal{F}(\mathcal{Z}_0 \mathfrak{S}'^{(l)}|_{\mathcal{Z}_0}), \mathcal{F}(\mathfrak{S}^{(l)}|_{\mathcal{Z}_0}) \{\mathbf{u}_0\} \rangle_{\mathcal{K}^{(l)}\{\mathbf{u}_0\}} (f, f') \\ & = \mathcal{F}_x \mathcal{F}_{x'} \left(\langle \mathcal{Z}_0 \mathfrak{S}'^{(l)}|_{\mathcal{Z}_0}, \mathfrak{S}^{(l)}|_{\mathcal{Z}_0} \rangle_{\mathcal{K}^{(l)}\{\mathbf{u}_0\}} \right) (f, f') \\ & = \mathcal{F}_x \mathcal{F}_{x'} \left(\langle \mathcal{Z}_0 H(\mathcal{Z}_0)(x), \mathfrak{S}^{(l)}|_{\mathcal{Z}_0}(x') \rangle \right) (f, f') \\ & = \mathcal{F}_x \mathcal{F}_{x'} \left(\langle \mathfrak{S}^{(l)}|_{\mathcal{Z}_0}(x), \mathfrak{S}^{(l)}|_{\mathcal{Z}_0}(x') \rangle \right) (f, f'). \end{aligned}$$

So, for parallel susceptibility we get following simple result:

$$\begin{aligned}\chi_{\parallel}(f, f') &= \frac{C_{R^{(l+1)}} \left(\langle \mathcal{F}(\mathcal{Z}_0 \mathfrak{S}'^{(l)}|_{\mathcal{Z}_0}), \mathcal{F}(\mathfrak{S}^{(l)}|_{\mathcal{Z}_0}) \{ \mathbf{u}_0 \} \rangle_{\mathcal{K}^{(l)} \{ u_0 \}} + \langle \mathcal{F}(\mathfrak{S}^{(l)}|_{\mathcal{Z}_0}), \mathcal{F}(\mathcal{Z}_0 \mathfrak{S}'^{(l)}|_{\mathcal{Z}_0}) \rangle_{\mathcal{K}^{(l)} \{ u_0 \}} \right)}{2\mathcal{K}^{(l)} \{ \mathbf{u}_0 \}} \\ &= \frac{\mathcal{K}^{(l+1)}(f, f')}{\mathcal{K}^{(l)}(f, f')}.\end{aligned}$$

And for the reduced perpendicular susceptibility:

$$\begin{aligned}\tilde{\chi}_{\perp}(f, f') &= \langle \mathcal{F}(\mathfrak{S}'^{(l)} \{ \mathbf{u}_0 \}), \mathcal{F}(\mathfrak{S}'^{(l)} \{ \mathbf{u}_0 \}) \rangle_{\mathcal{K}^{(l)} \{ u_0, u_0 \}} \\ &= \mathcal{F}_x \mathcal{F}_{x'} \left(\left\| \left((\alpha - \beta) H(x) + \beta \right) \right\|_{\mathcal{K}^{(l)} \{ u_0, u_0 \}} \right) \\ &= \mathcal{F}_x \mathcal{F}_{x'} \left(\frac{(\alpha - \beta)^2}{4} \left(1 + \frac{2}{\pi} \arcsin \rho \right) + \alpha \beta \right).\end{aligned}$$

Theorem 2 With the scale-invariant activation specified in Eq. (35) and a Fourier Neural Operator defined by Eq. (9) under the initialization ensemble (10), the kernel and the susceptibilities are given by the following recursion relations:

$$\begin{aligned}\mathcal{K}^{(l+1)}(f, f') &= (\alpha - \beta)^2 \delta(f - f') C_{R^{(l+1)}}(f) \int \int \frac{V^{(l)}}{4\pi} (2\sqrt{1 - (\rho^{(l)})^2} + \rho^{(l)}(\pi + 2 \arcsin \rho^{(l)})) e^{-ifx + if'x'} dx dx' \\ &\quad + \alpha \beta \delta(f - f') C_{R^{(l+1)}}(f) \mathcal{H}^{(l)}(f, f'), \\ \int \mathcal{K}^{(l+1)}(f, f') df df' &= \frac{\alpha^2 + \beta^2}{2} \int \mathcal{H}^{(l)}(f) df \\ \chi_{\parallel}(f, f') &= \frac{\mathcal{K}^{(l+1)}(f, f')}{\mathcal{K}^{(l)}(f, f')}, \\ \tilde{\chi}_{\perp}(f, f') &= \mathcal{F}_x \mathcal{F}_{x'} \left(\frac{(\alpha - \beta)^2}{4} \left(1 + \frac{2}{\pi} \arcsin \rho \right) + \alpha \beta \right).\end{aligned}$$

where $V^{(l)} = \int \mathcal{H}^{(l)}(f) df$, $V^{(l)} \rho^{(l)}(x, x') = \int \mathcal{H}^{(l)} \cos(f(x - x')) df$.

4.3 Architecture with Residual Connection

The practical implementation of the FNO does not retain the full spectrum; instead, all modes above a prescribed cut-off are truncated after performing the FFT. When no activation is applied—that is, every layer remains linear—the pre-activations and the final output are computed entirely within this truncated spectral band. By contrast, once a non-linear activation is introduced, the analysis in sections 4.1–4.2 shows that low-frequency components become coupled to high-frequency kernels; the experiments in Section 5 confirm the same phenomenon empirically. For inputs of modest spatial extent and operators with large channel width, the kernel recursion equation in Theorem 1 implies that non-linearity-induced frequency coupling is weak. To preserve the computational gains of spectral truncation while still accumulating the necessary non-linear interactions, the network is modified into a ResNet-style architecture: the pre-activation of each layer is added back to its activation output, forming a residual connection. This design is expected to (i) mitigate the

attenuation of high-frequency information as depth increases and (ii) allow the neural operator to process fine-scale features more effectively. The remainder of this section develops the accompanying theoretical framework for FNOs with such residual connections. Firstly, we define the weighted residual connection for the kernel integration layer. We modify the Eq. (9) as follows:

$$\mathcal{Z}^{(l+1)}(u) := \mathcal{R}^{(l+1)}(\mathfrak{S}^{(l)}(u)) + \tilde{\gamma} \mathcal{Z}^{(l)}(u). \quad (45)$$

where $\tilde{\gamma}$ is a hyperparameter to be set. Then the recursive kernel for residual connection architecture is modified as follows:

$$\mathcal{K}^{(l+1)}\{\mathbf{u}, \mathbf{v}\}(f) := \langle \mathcal{R}^{(l+1)}(\mathcal{F}(\mathfrak{S}^{(l)}\{\mathbf{u}\}) + \tilde{\gamma} \mathcal{Z}^{(l)}\{\mathbf{u}\}), \mathcal{F}(\mathcal{R}^{(l+1)}(\mathfrak{S}^{(l)}\{\mathbf{v}\}) + \tilde{\gamma} \mathcal{Z}^{(l)}\{\mathbf{v}\}) \rangle_{\mathcal{K}^{(l)}}$$

Then, for single input data, we get the following recursive formula:

$$\begin{aligned} \mathcal{K}^{(l+1)}\{\mathbf{u}\}(f) &:= C_{R^{(l+1)}} \|\mathcal{F}(\mathfrak{S}^{(l)}\{\mathbf{u}\})\|_{\mathcal{K}^{(l)}} + \tilde{\gamma} \langle \mathcal{F}(\mathcal{Z}^{(l)}\{\mathbf{u}\}), \mathcal{F}(\mathfrak{S}^{(l+1)}\{\mathbf{u}\}) \rangle_{\mathcal{K}^{(l)}} \\ &+ \tilde{\gamma} \langle \mathcal{F}(\mathfrak{S}^{(l+1)}\{\mathbf{u}\}), \mathcal{F}(\mathcal{Z}^{(l)}\{\mathbf{u}\}) \rangle_{\mathcal{K}^{(l)}} + \tilde{\gamma}^2 \|\mathcal{F}(\mathcal{Z}^{(l)}\{\mathbf{u}\})\|_{\mathcal{K}^{(l)}} \end{aligned}$$

then for analytic activation case, we have following kernel recursive formula:

$$\begin{aligned} \mathcal{K}^{(l+1)}\{\mathbf{u}\}(f) &= \delta(f - f') \left((\sigma_1^2 C_{R^{(l+1)}}(f) + \gamma) \mathcal{K}^{(l)}\{\mathbf{u}\}(f) \right. \\ &+ \sum_{k=2}^{\infty} \frac{\sigma_k^2}{(n^{(l)})^k} \sum_{n_{k,1}+\dots+n_{k,l}=k} \frac{(n_{k,1})! \dots (n_{k,l})!}{k!} (\mathcal{H}^{(l)})^{*n_{k,1}} \dots (\mathcal{H}^{(l)})^{*n_{k,l}}(f) \left. \right). \\ &\langle \mathcal{F}(\mathcal{Z}^{(l)}\{\mathbf{u}_0\}) \mathfrak{S}'^{(l+1)}\{\mathbf{u}_0\} + \tilde{\gamma} \mathcal{Z}^{(l)}\{\mathbf{u}_0\}, \mathcal{F}(\mathfrak{S}^{(l)}\{\mathbf{u}_0\}) + \tilde{\gamma} \mathcal{Z}^{(l)}\{\mathbf{u}_0\} \rangle_{\mathcal{K}^{(l)}\{\mathbf{u}_0, \mathbf{u}_0\}} \\ &= \langle \mathcal{F}(\mathcal{Z}^{(l)}\{\mathbf{u}_0\}) \mathfrak{S}'^{(l+1)}\{\mathbf{u}_0\}, \mathcal{F}(\mathfrak{S}^{(l+1)}\{\mathbf{u}_0\}) \rangle_{\mathcal{K}^{(l)}\{\mathbf{u}_0, \mathbf{u}_0\}} + \tilde{\gamma} \langle \mathcal{F}(\mathcal{Z}^{(l)}\{\mathbf{u}_0\}), \mathcal{F}(\mathfrak{S}^{(l)}\{\mathbf{u}_0\}) \rangle_{\mathcal{K}^{(l)}\{\mathbf{u}_0, \mathbf{u}_0\}} \\ &+ \tilde{\gamma} \langle \mathcal{F}(\mathcal{Z}^{(l)}\{\mathbf{u}_0\}) \mathfrak{S}'^{(l)}\{\mathbf{u}_0\}, \mathcal{F}(\mathcal{Z}^{(l)}\{\mathbf{u}_0\}) \rangle_{\mathcal{K}^{(l)}\{\mathbf{u}_0, \mathbf{u}_0\}} + \tilde{\gamma}^2 \|\mathcal{F}(\mathcal{Z}^{(l)}\{\mathbf{u}_0\})\|_{\mathcal{K}^{(l)}} \\ &= \delta(f - f') \left(\gamma \mathcal{K}^{(l)}\{\mathbf{u}\}(f) + C_{R^{(l+1)}}(f) \sum_{k=1}^{\infty} \frac{\sigma_k^2}{(n^{(l)})^{k-1}} \sum_{n_{k,1}+\dots+n_{k,l}=k} \frac{k(n_{k,1})! \dots (n_{k,l})!}{(k-1)!} (\mathcal{H}^{(l)})^{*n_{k,1}} \dots (\mathcal{H}^{(l)})^{*n_{k,l}}(f) \right) \end{aligned} \quad (46)$$

where $\gamma = \tilde{\gamma}^2$. And for susceptibilities we calculate similarly:

$$\begin{aligned} &\langle \mathcal{F}(\mathfrak{S}'^{(l)}\{\mathbf{u}_0\} + \tilde{\gamma}), \mathcal{F}(\mathfrak{S}'^{(l)}\{\mathbf{u}_0\} + \tilde{\gamma}) \rangle_{\mathcal{K}^{(l)}\{\mathbf{u}_0, \mathbf{u}_0\}} \\ &= \langle \mathcal{F}(\mathfrak{S}'^{(l)}\{\mathbf{u}_0\}), \mathcal{F}(\mathfrak{S}'^{(l)}\{\mathbf{u}_0\}) \rangle_{\mathcal{K}^{(l)}\{\mathbf{u}_0, \mathbf{u}_0\}} + 2 \langle \mathcal{F}(\mathfrak{S}'^{(l)}\{\mathbf{u}_0\}), \tilde{\gamma} \rangle_{\mathcal{K}^{(l)}\{\mathbf{u}_0, \mathbf{u}_0\}} + \gamma \delta(f) \delta(f') \\ &= \left(\sum_{k=1}^{\infty} \frac{\sigma_k^2}{(n^{(l)})^{k-1}} \sum_{n_{k,1}+\dots+n_{k,l}=k-1} \frac{(n_{k,1})! \dots (n_{k,l})!}{(k-1)!} (\mathcal{H}^{(l)})^{*n_{k,1}} \dots (\mathcal{H}^{(l)})^{*n_{k,l}}(f) \right) \\ &+ \gamma \delta(f) \delta(f'). \end{aligned} \quad (47)$$

Theorem 3 With the analytic, origin-passing activation specified in Eq. (32) and a Fourier Neural Operator defined based on Eq. (9) and modification of Fourier layers by Eq. (45)

under the initialization ensemble (10), the kernel and the susceptibilities are given by the following recursion relations:

$$\begin{aligned}
\mathcal{K}^{(l+1)}\{\mathbf{u}\}(f) &= \delta(f - f') \left((\sigma_1^2 C_{R^{(l)}}(f) + \gamma) \mathcal{K}^{(l)}\{\mathbf{u}\}(f) \right. \\
&\quad \left. + \sum_{k=2}^{\infty} \frac{\sigma_k^2}{(n^{(l)})^{k-1}} \sum_{n_{k,1}+\dots+n_{k,l}=k} \frac{(n_{k,1})! \dots (n_{k,l})!}{k!} (\mathcal{H}^{(l)})^{*n_{k,1}} \dots (\mathcal{H}^{(l)})^{*n_{k,l}}(f) \right). \\
\chi_{\parallel}(f, f') &= \delta(f - f') \left(\gamma + C_{R^{(l+1)}}(f) \sum_{k=1}^{\infty} \frac{\sigma_k^2}{(n^{(l)})^{k-1}} \sum_{n_{k,1}+\dots+n_{k,l}=k} \frac{k(n_{k,1})! \dots (n_{k,l})!}{(k-1)!} \frac{(\mathcal{H}^{(l)})^{*n_{k,1}} \dots (\mathcal{H}^{(l)})^{*n_{k,l}}(f)}{\mathcal{K}^{(l)}\{\mathbf{u}_0\}} \right). \\
\tilde{\chi}_{\perp}(f, f') &= \left(\sum_{k=1}^{\infty} \frac{\sigma_k^2}{(n^{(l)})^{k-1}} \sum_{n_{k,1}+\dots+n_{k,l}=k-1} \frac{(n_{k,1})! \dots (n_{k,l})!}{(k-1)!} (\mathcal{H}^{(l)})^{*n_{k,1}} \dots (\mathcal{H}^{(l)})^{*n_{k,l}}(f) \right) \\
&\quad + (\gamma + 2\tilde{\gamma}\sigma_1)\delta_{f,f'}.
\end{aligned}$$

4.4 On the Compact Periodic Domain

As noted above, when the domain is the entire real line, the formula in Lemma 2 yields a $\delta(0)$ term—i.e., a divergent value. In practice, however, we implement the FNO on a finite periodic domain, and in this setting the $\delta(0)$ in equations in previous sections equals to $\frac{1}{L}$ where L is size of the domain, so the divergence disappears. Consequently, the kernel-evolution equations and criticality conditions in Sections 4.1, 4.2, and 4.3 can be rewritten as follows:

Corollary 1 With the analytic, origin-passing activation specified in Eq. (32) and a Fourier Neural Operator defined by Eq. (9) under the initialization ensemble (10), the kernel and the susceptibilities are given by the following recursion relations:

$$\mathcal{K}^{(l+1)}(m, n) = \frac{\delta_{m,n}}{L} \sum_{k=1}^{\infty} \frac{\sigma_k^2}{(n^{(l)})^{k-1}} \sum_{n_{k,1}+\dots+n_{k,l}=k} \frac{(n_{k,1})! \dots (n_{k,l})!}{k!} (\mathcal{H}^{(l)})^{*n_{k,1}} \dots (\mathcal{H}^{(l)})^{*n_{k,l}}(f) \quad (48)$$

$$\chi_{\parallel}(m, n) = \frac{\delta_{m,n}}{L} C_{R^{(l+1)}} \sum_{k=1}^{\infty} \frac{\sigma_k^2}{(n^{(l)})^{k-1}} \sum_{n_{k,1}+\dots+n_{k,l}=k} \frac{(n_{k,1})! \dots (n_{k,l})!}{(k-1)!} \frac{(\mathcal{H}^{(l)})^{*n_{k,1}} \dots (\mathcal{H}^{(l)})^{*n_{k,l}}(f)}{\mathcal{K}^{(l)}\{\mathbf{u}_0\}(f)}, \quad (49)$$

$$\tilde{\chi}_{\perp}(m, n) = \sum_{k=1}^{\infty} \frac{\sigma_k^2}{(n^{(l)})^{k-1}} \sum_{n_{k,1}+\dots+n_{k,l}=k-1} \frac{(n_{k,1})! \dots (n_{k,l})!}{(k-1)!} (\mathcal{H}^{(l)})^{*n_{k,1}} \dots (\mathcal{H}^{(l)})^{*n_{k,l}}(f). \quad (50)$$

Corollary 2 With the scale-invariant activation specified in Eq. (35) and a Fourier Neural Operator defined by Eq. (9) under the initialization ensemble (10), the kernel and the

susceptibilities are given by the following recursion relations:

$$\begin{aligned}\mathcal{K}^{(l+1)}(m, n) &= (\alpha - \beta)^2 \int \int \frac{V^{(l)}}{4\pi} (2\sqrt{1 - (\rho^{(l)})^2} + \rho^{(l)}(\pi + 2 \arcsin \rho^{(l)}) e^{-imx+inx'} dx dx' \\ &\quad + \alpha\beta \frac{\delta_{m,n}}{L} \mathcal{H}^{(l)}(m, n)),\end{aligned}\tag{51}$$

$$\sum_n \mathcal{K}^{(l+1)}(n) = \frac{\alpha^2 + \beta^2}{2} \sum_n \mathcal{H}^{(l)}(n)\tag{52}$$

$$\chi_{\parallel}(m, n) = \frac{\mathcal{K}^{(l+1)}(m, n)}{\mathcal{K}^{(l)}(m, n)},\tag{53}$$

$$\tilde{\chi}_{\perp}(m, n) = \int \left(\frac{(\alpha - \beta)^2}{4} \left(1 + \frac{2}{\pi} \arcsin \rho \right) + \alpha\beta \right) e^{-imx+inx'} dx dx'.\tag{54}$$

where $V^{(l)} = \sum_n \mathcal{K}^{(l)}(n)$, $V^{(l)} \rho^{(l)}(x, x') = \sum_n \mathcal{H}^{(l)}(n) \cos(n(x - x'))$.

Corollary 3 With the analytic, origin-passing activation specified in Eq. (32) and a Fourier Neural Operator defined based on Eq. (9) and modification of Fourier layers by Eq. (45) under the initialization ensemble (10), the kernel and the susceptibilities are given by the following recursion relations:

$$\begin{aligned}\mathcal{K}^{(l+1)}\{\mathbf{u}\}(m, n) &= \frac{\delta_{m,n}}{L} \left((\sigma_1^2 C_{R^{(l)}}(n) + \gamma) \mathcal{K}^{(l)}\{\mathbf{u}\}(n) \right. \\ &\quad \left. + \sum_{k=2}^{\infty} \frac{\sigma_k^2}{(n^{(l)})^{k-1}} \sum_{n_{k,1}+\dots+n_{k,l}=k} \frac{(n_{k,1})! \dots (n_{k,l})!}{k!} (\mathcal{H}^{(l)})^{*n_{k,1}} \dots (\mathcal{H}^{(l)})^{*n_{k,l}}(n) \right).\end{aligned}\tag{55}$$

$$\begin{aligned}\chi_{\parallel}(m, n) &= \frac{\delta_{m,n}}{L} \left(\gamma + C_{R^{(l+1)}}(n) \right. \\ &\quad \left. + \sum_{k=1}^{\infty} \frac{\sigma_k^2}{(n^{(l)})^{k-1}} \sum_{n_{k,1}+\dots+n_{k,l}=k} \frac{k(n_{k,1})! \dots (n_{k,l})!}{(k-1)!} \frac{(\mathcal{H}^{(l)})^{*n_{k,1}} \dots (\mathcal{H}^{(l)})^{*n_{k,l}}(n)}{\mathcal{K}^{(l)}\{\mathbf{u}_0\}} \right).\end{aligned}\tag{56}$$

$$\begin{aligned}\tilde{\chi}_{\perp}(m, n) &= \left(\sum_{k=1}^{\infty} \frac{\sigma_k^2}{(n^{(l)})^{k-1}} \sum_{n_{k,1}+\dots+n_{k,l}=k-1} \frac{(n_{k,1})! \dots (n_{k,l})!}{(k-1)!} (\mathcal{H}^{(l)})^{*n_{k,1}} \dots (\mathcal{H}^{(l)})^{*n_{k,l}}(n) \right) + \gamma \sigma_1 \delta_{n,m}.\end{aligned}\tag{57}$$

5. Experimental Validations

In this section we empirically validate the theoretical findings from Section 4 and illustrate how they can be exploited in practice. We run three complementary sets of experiments. First, we verify qualitatively that a non-linear activation couples low and high frequencies, and then test the theory quantitatively by predicting the next-layer kernel from the current one via Eqs. (48), (51) and (55) and comparing that prediction with measurements. Next, under fixed hyper-parameters, we experimentally confirm that the susceptibilities in the Fourier layers behave as our theory predicts.

5.1 Kernel Evolution Prediction

In this subsection we start by examining how the kernel evolves under three different activations—quadratic, tanh, and ReLU—across a range of network depths and widths. We then study how the kernel changes when a tanh activation is used inside a ResNet-style FNO. Finally, using the kernel-recursion formula derived in Section 4, we feed the empirical kernel from layer l into the recurrence to predict the kernel at layer $l+1$ and compare that prediction with the measured kernel. To validate the frequency coupling and theoretical prediction over the truncation frequency (k_{\max}), we consider the reduced kernel $\tilde{\mathcal{K}}$ which is defined as follows:

$$\tilde{\mathcal{K}}^{(l+1)}\{\mathbf{u}, \mathbf{v}\}(f, f') := \langle \mathcal{F}(\mathfrak{S}^{(l)}\{\mathbf{u}\}), \mathcal{F}(\mathfrak{S}^{(l)}\{\mathbf{v}\}) \rangle_{\mathcal{K}^{(l)}}(f, f').$$

Figures 1–4 compare the statistics of networks with and without a nonlinear activation. In every run we set $C_R = 1$ and examined two width–depth pairs, $(4, 64)$ and $(2, 4)$. Inputs were sampled from the mean-zero Gaussian random field with covariance $C(x, y) \sim e^{-\|x-y\|^2/K^2}$, and the spectral truncation wavenumber was fixed at 32. For each configuration we initialised 100 independent models. We then plotted, on a logarithmic scale, the kernel value at each frequency, i.e., the squared magnitude of the Fourier transform of the output layer. Each dot represents a single model, while the thick line is the log of the kernel averaged over all 100 models. Figure 1 shows the case with the quadratic activation $\sigma(x) = x^2 + x$. When the activation is absent the kernel drops to zero—within numerical error—exactly after the truncation frequency, but once the activation is applied non-zero energy remains up to twice the truncation frequency, a direct consequence of the second, double-convolution term in the recursion formula. Figure 2 uses tanh, an analytic function, and because every term in its Taylor series contributes, the frequency-coupling effect survives at much higher wavenumbers. Figure 3 employs the non-analytic ReLU; here the kernel decays only slowly beyond the truncation point even if residual connection is absent, which is explained by the theory: the next-layer kernel is the Fourier transform of $\rho^{(l)}(x, y)$, and the strong weight of $\rho^{(l)}$ near zero in position space spreads energy across the entire frequency axis. Figure 4 adds a residual connection with tanh activation; to prevent kernel blow-up the weight variance is scaled by $1 - \gamma$. With a small γ the kernel decays rapidly as depth increases, whereas a large γ leaves much of the high-frequency energy intact, exactly as predicted by the residual-criticality analysis. Across all four figures two patterns are evident. First, increasing the channel width pulls the kernels of individual models ever closer to the ensemble mean, confirming the theoretical $\frac{1}{\text{width}}$ suppression of the four-point vertex. Second, larger widths also reduce the absolute kernel magnitude at frequencies beyond the truncation threshold, again in quantitative agreement with the recursion formula. Figures 5, 6, 7 and 8 show that the kernels measured in the post-truncation frequency band (17 to 63) match the values predicted by our formulas. The experimental setup is the same as in Figures 1–4. We ran separate tests for the quadratic, cubic, ReLU and ResNet cases, fixing the channel width at 32 throughout. The shaded region in each plot marks one standard deviation across 100 independent runs, and in almost every plot the theoretical curve stays well inside that band. For the quadratic and cubic activations we report results at Fourier-layer depths 0 and 2; for the ReLU and ResNet cases we show depths 0, 1, 2 and 3. The cubic activation was tested in two versions: one containing only

the cubic term and another containing both the quadratic and cubic terms. To demonstrate that the agreement is not a coincidence that arises when only a single term is present, we performed ablation tests in which individual terms were removed from the activation and the theoretical kernel was recalculated. The plots make clear that agreement with the measurements is achieved only when all relevant terms are included in the theory.

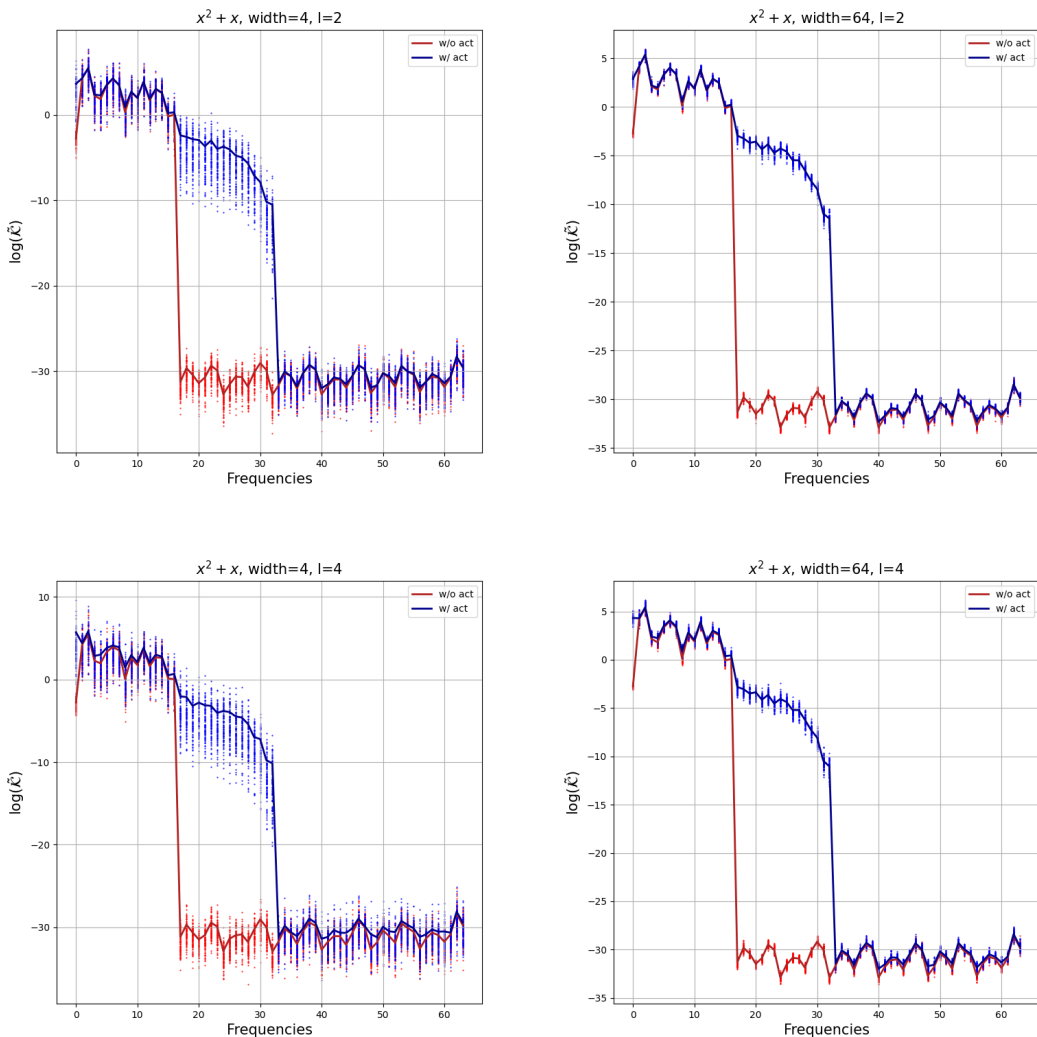


Figure 1: Log-scale plot of the reduced kernel for quadratic activation cases.

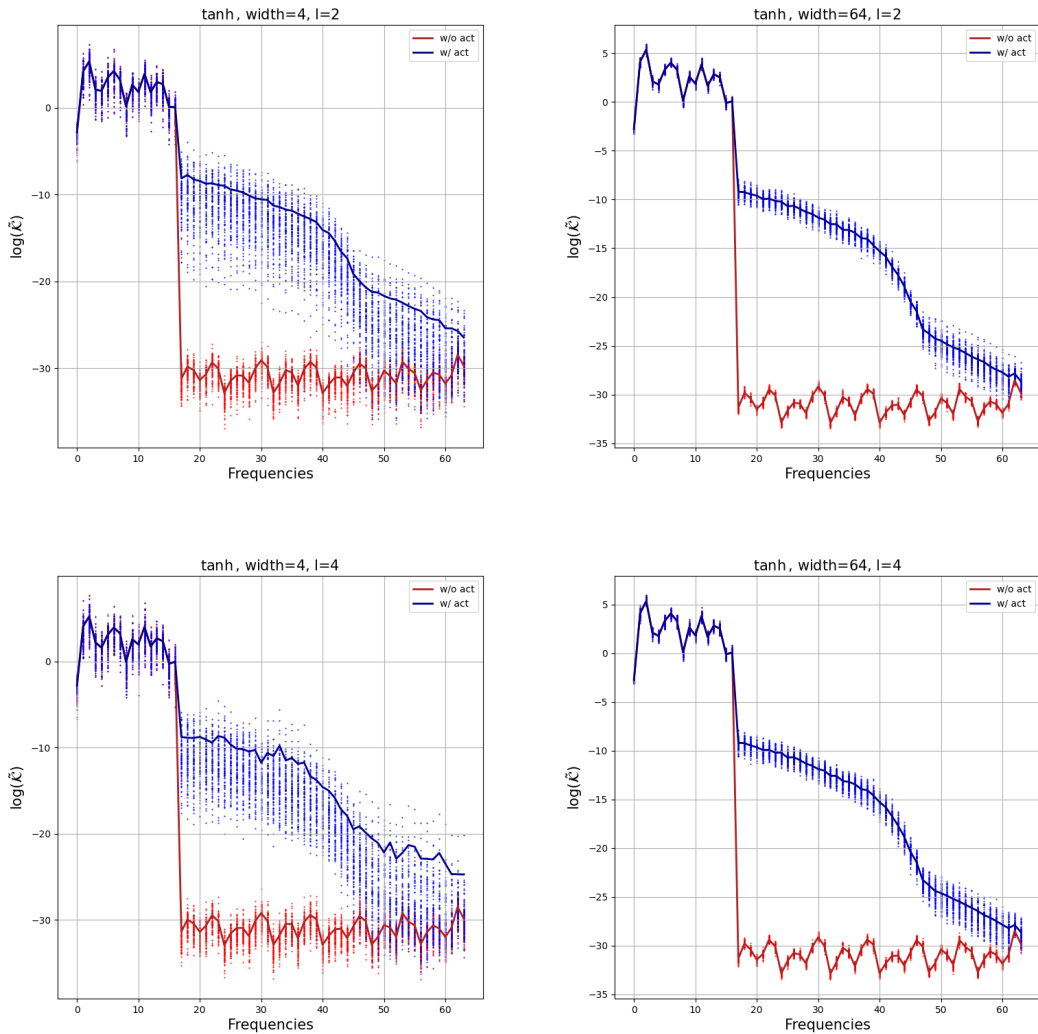


Figure 2: Log-scale plot of the reduced kernel for tanh activation cases.

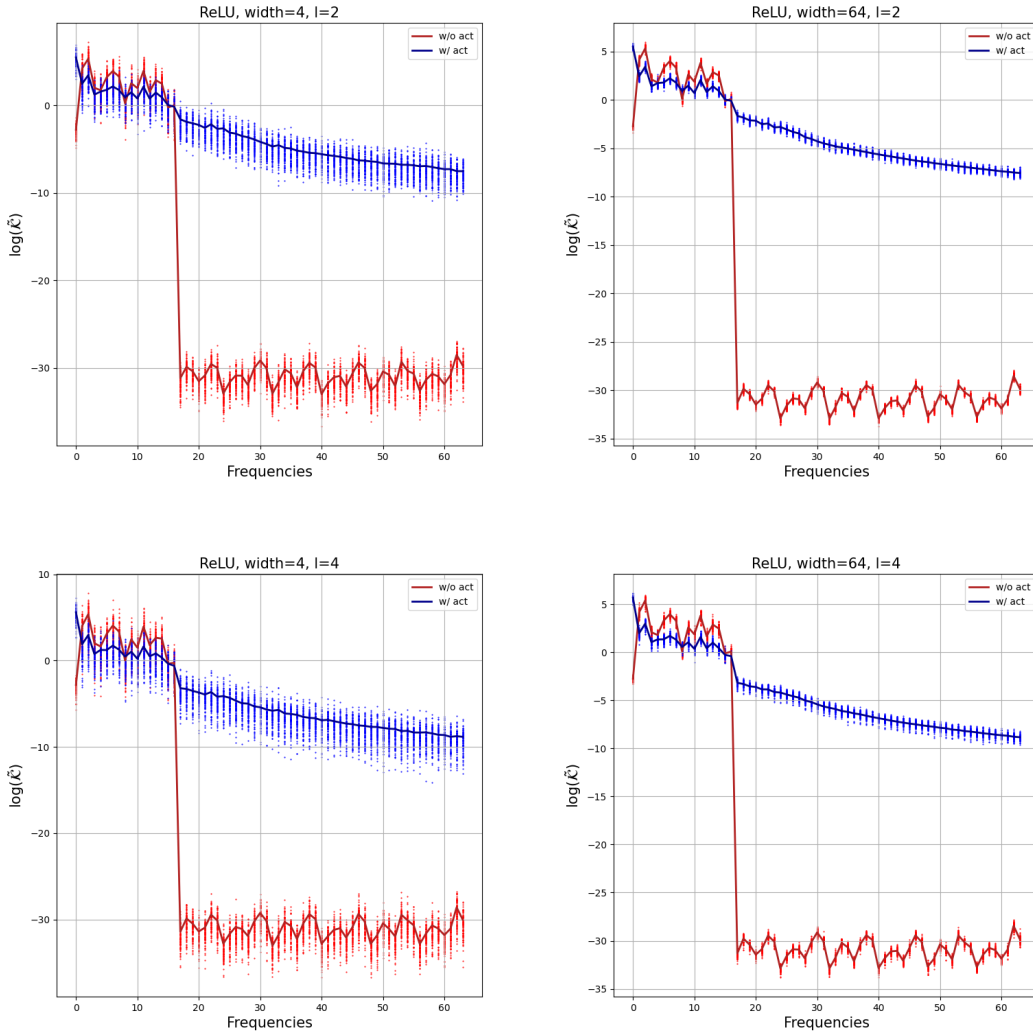


Figure 3: Log-scale plot of the reduced kernel for ReLU activation cases.

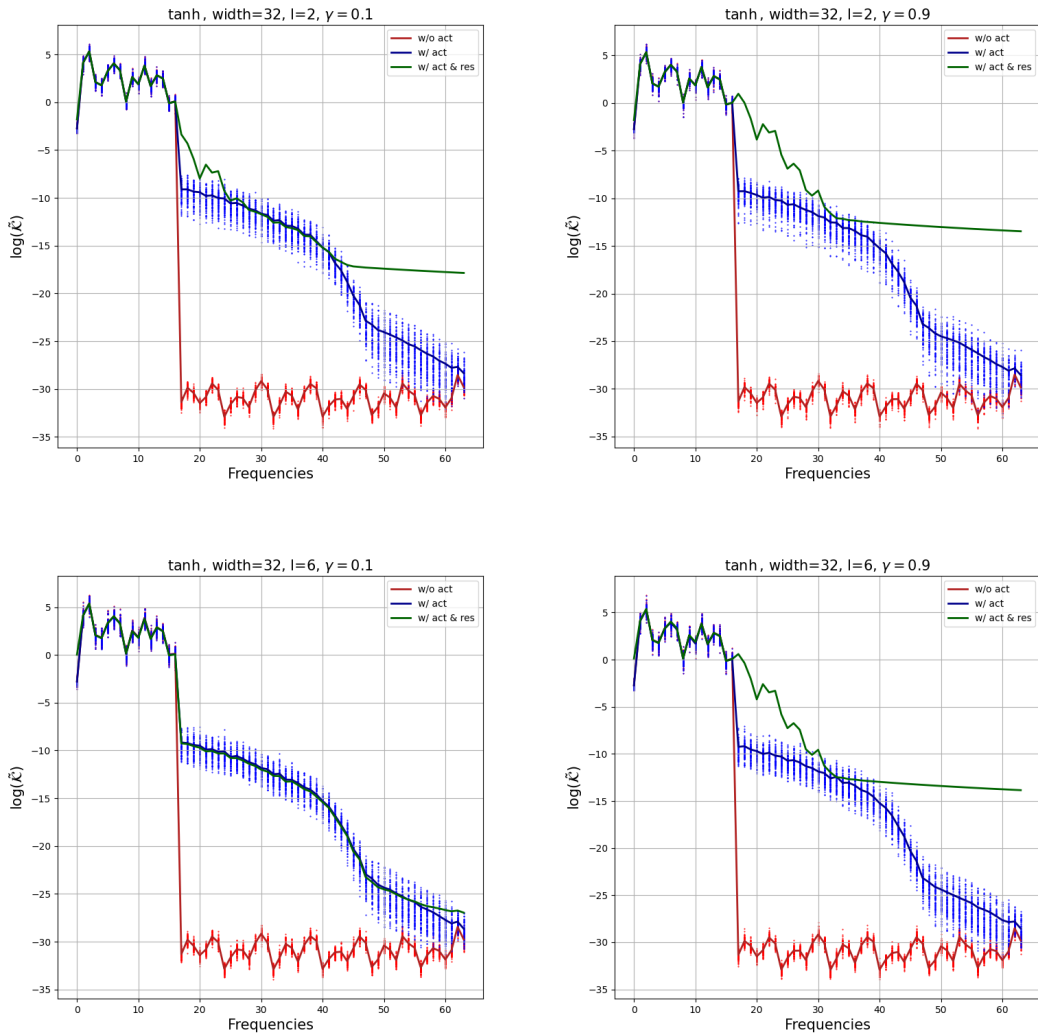


Figure 4: Log-scale plot of the reduced kernel for tanh activation cases with residual connections at weights $\gamma = 0.1$ and $\gamma = 0.9$.

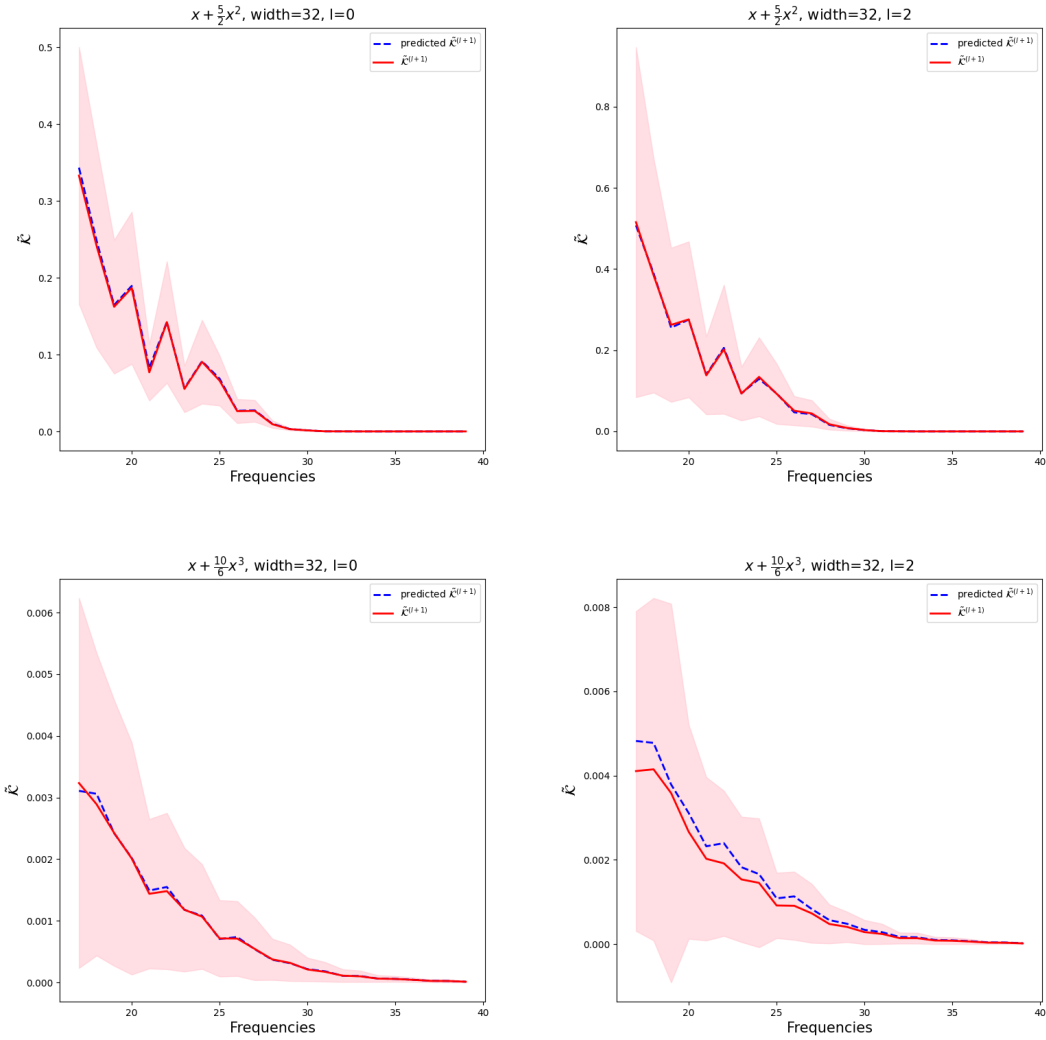


Figure 5: Comparison of empirical and theoretical kernel predictions for quadratic and cubic activations; pink area shows ± 1 standard deviation.

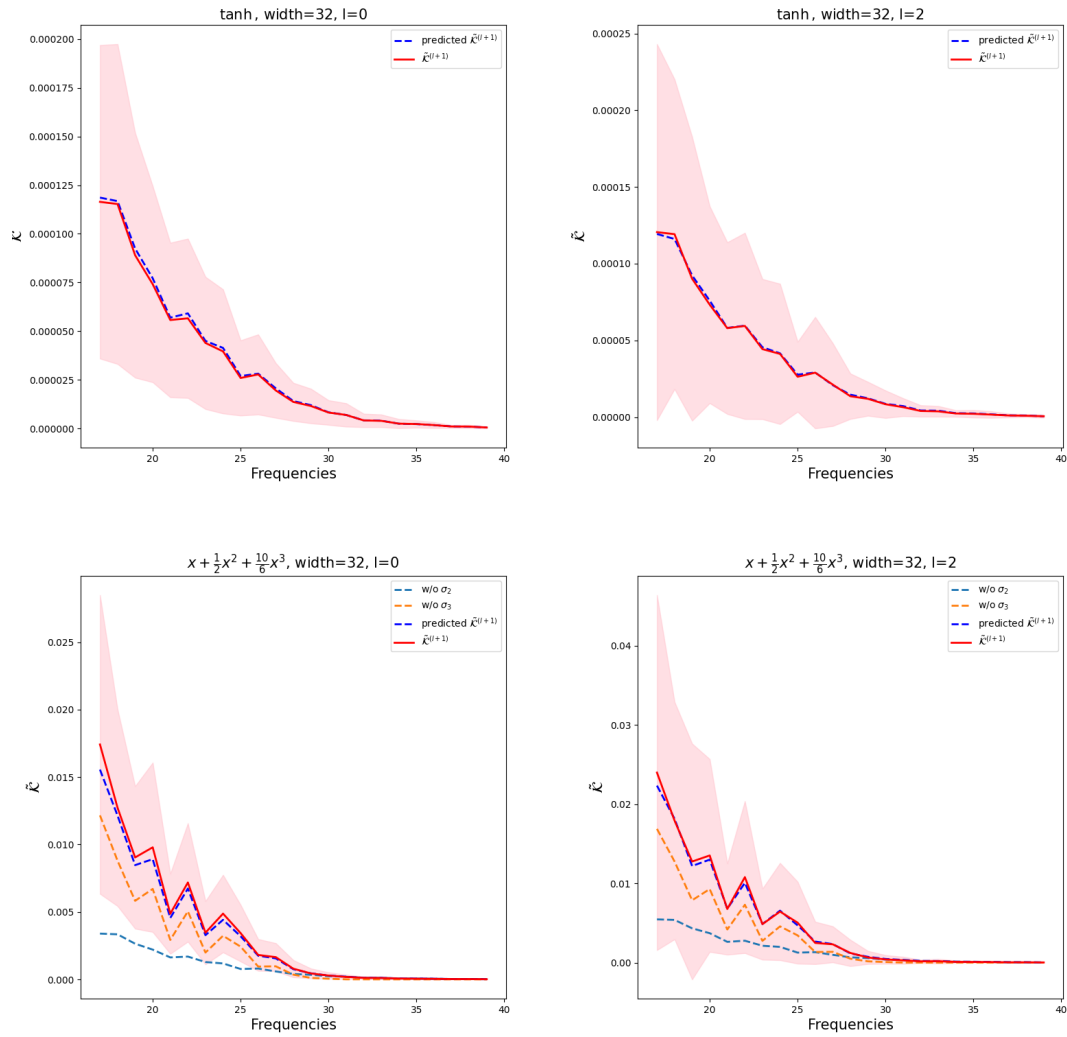


Figure 6: Comparison of empirical and theoretical kernel predictions for tanh and cubic with quadratic term activations; pink area shows ± 1 standard deviation.

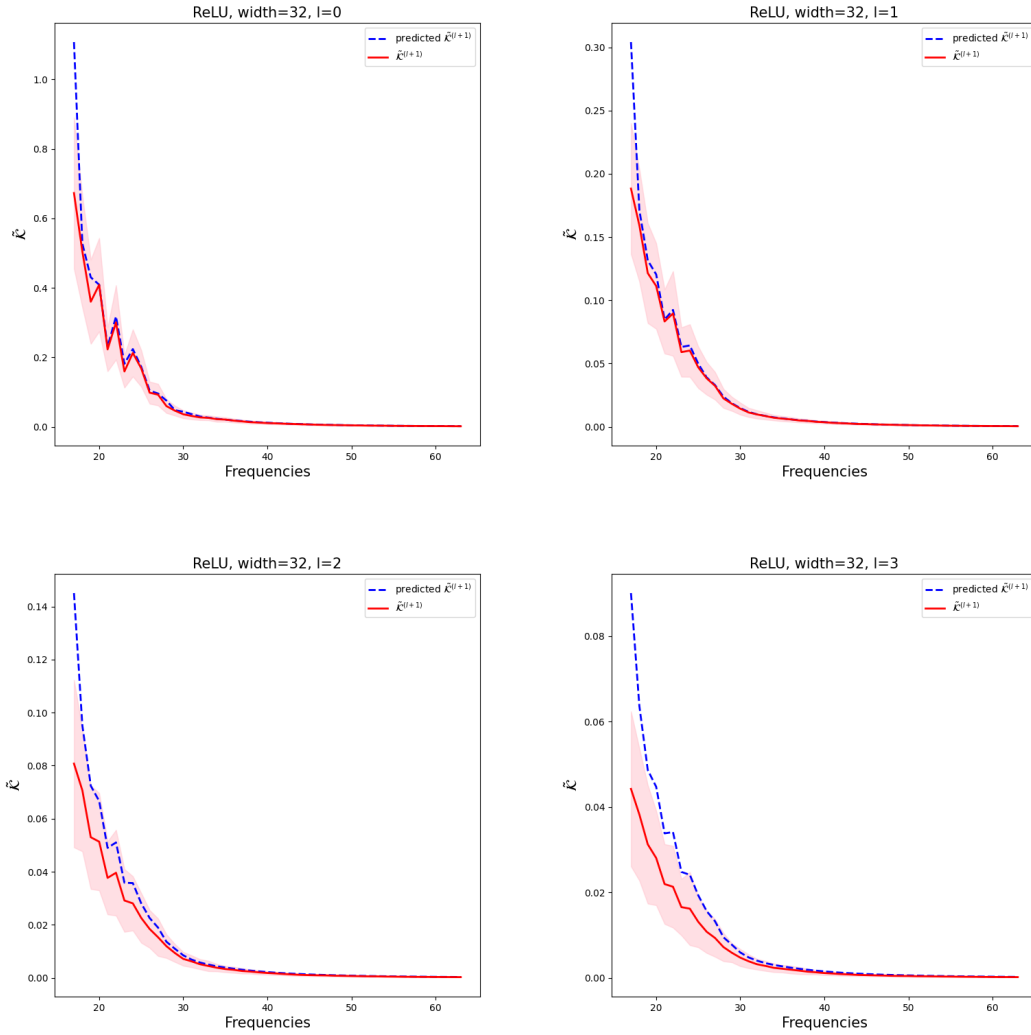


Figure 7: Comparison of empirical and theoretical kernel predictions for ReLU activation; pink area shows ± 1 standard deviation.

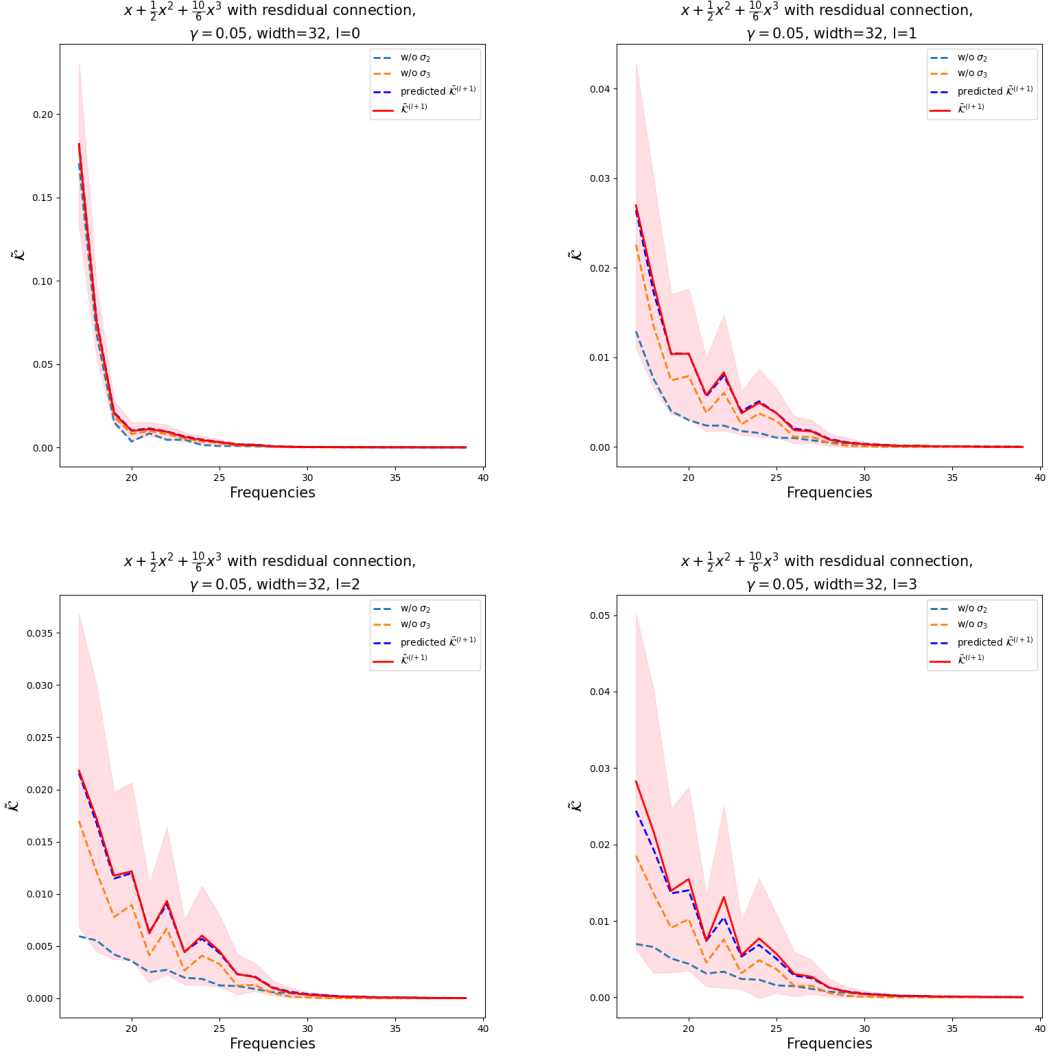


Figure 8: Comparison of empirical and theoretical kernel predictions for cubic with quadratic term activations with residual connection at weight $\gamma = 0.05$; pink area shows ± 1 standard deviation.

5.2 Susceptibility Prediction

This section tests the parallel and perpendicular susceptibilities predicted by our theory. We use the same architecture throughout: truncation frequency 32, channel width 32, and inputs drawn from the Gaussian field distribution used earlier. For each model we measure the first Fourier-layer output. In the parallel case we add a perturbation of size $\epsilon = 0.01$ in the data-direction specified by the theory, follow the prescription of Eqs. (49), (53) and (56) to compute the susceptibility at every frequency, and average over one hundred independently initialised networks. For the perpendicular case we inject an orthogonal perturbation of size $\epsilon = 1e - 5$, integrate the resulting power across the full frequency range as dictated by Eqs. (50), (54) and (57), and again average over a hundred runs. We evaluate four activation settings: quadratic, cubic, ReLU, and—in a ResNet variant—a cubic activation with residual gain $\gamma = 0.25$ and $\gamma = 0.75$. The ReLU susceptibilities are predicted from Eqs. (53) and (54), while those for the ResNet come from Eqs. (56) and (57). In every case the weight-variance profile $C_R(f)$ is a step function that drops to zero above $k_{\max} = 32$. For the parallel tests we fix C_R to 1, while in the perpendicular tests we sweep C_R between 0.80 and 1.20. Because the non-ResNet models have zero kernel beyond the truncation frequency, results for those runs are shown only up to k_{\max} ; the ResNet retains energy beyond the cutoff, so we plot its curves out to twice k_{\max} . Figures 9 and 10 reveal close agreement between theory and measurement: the empirical susceptibilities stay within one standard deviation of the predicted curves across all activations, perturbation types, and depths.

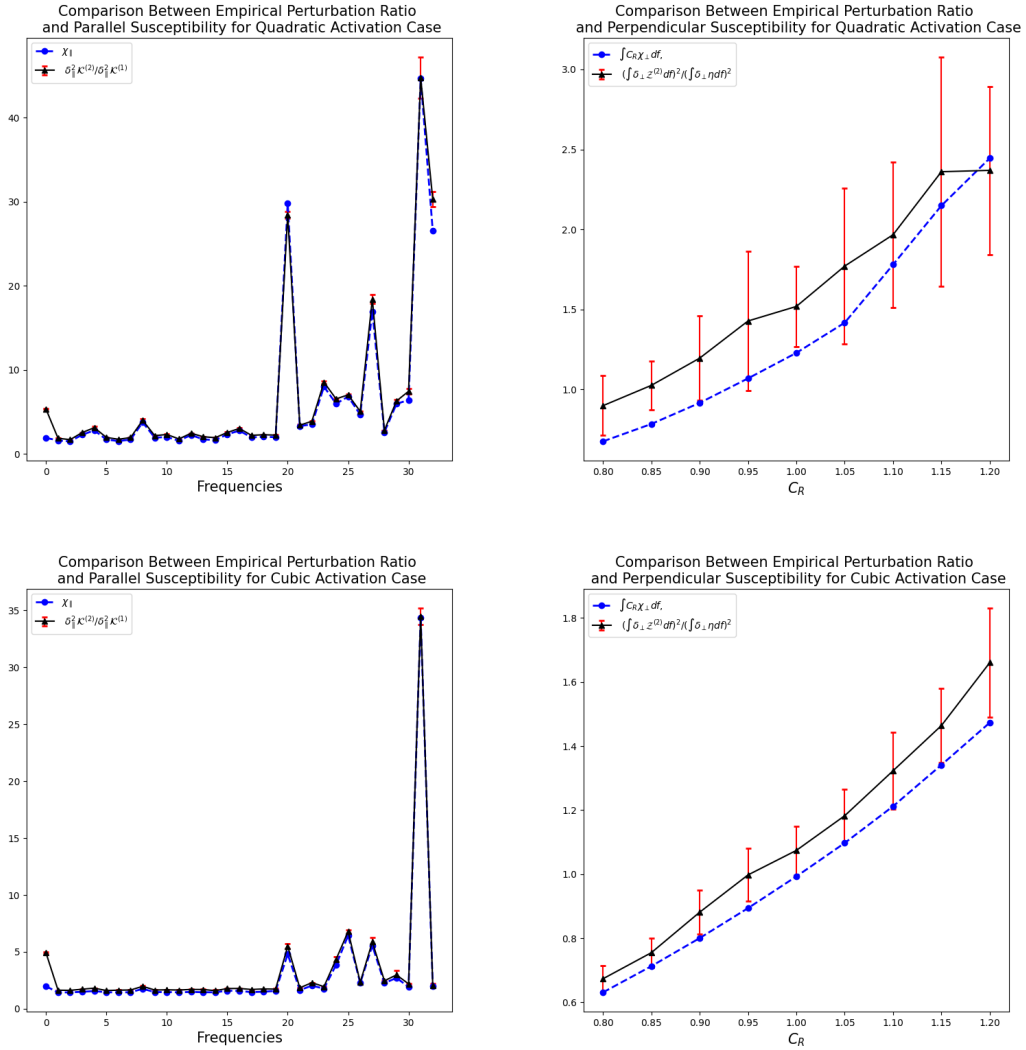
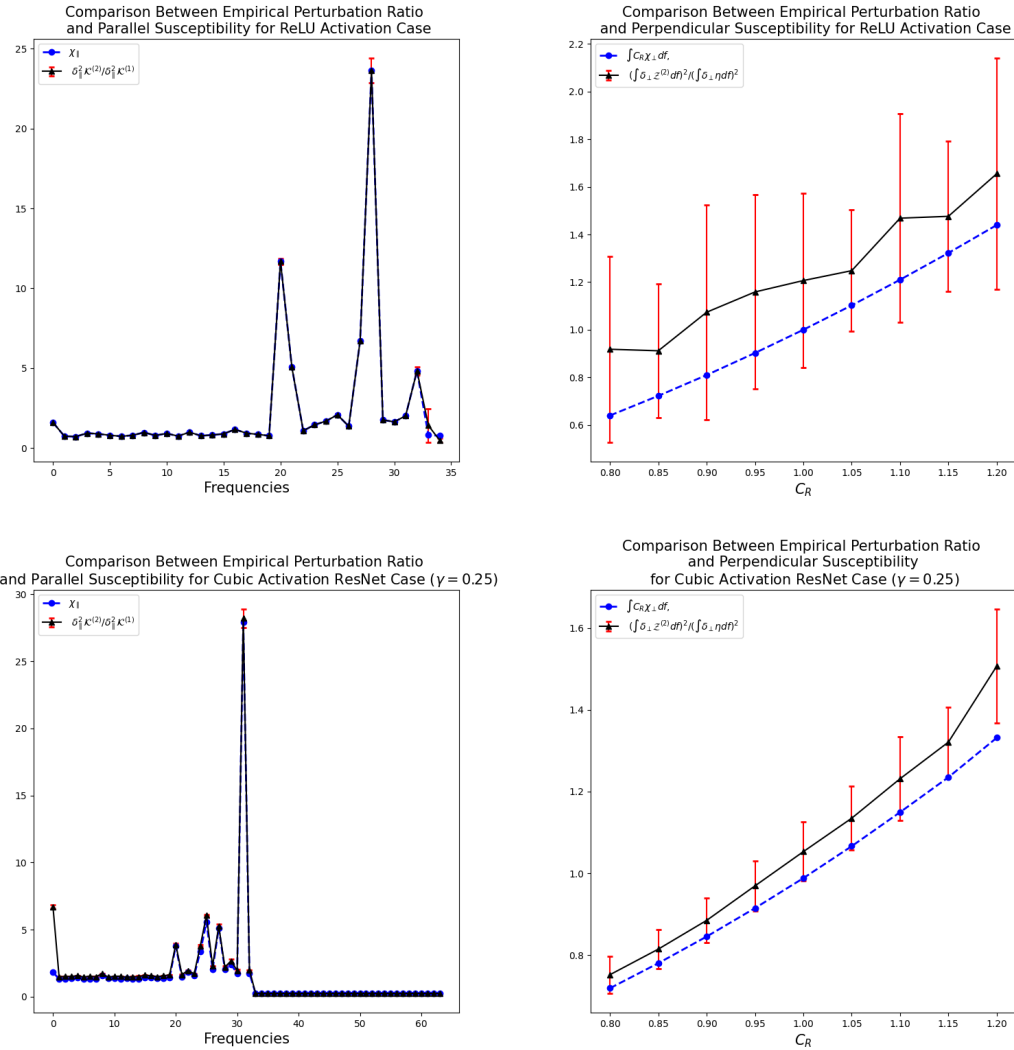


Figure 9: Comparison of empirical and theoretical susceptibility predictions for quadratic and cubic activations; red error bars show ± 1 standard deviation. (Left: parallel susceptibility, Right: perpendicular susceptibility)

6. Conclusion

This study analyzes neural operators for functional data directly in function space—without recasting the problem through discretization—by examining their kernels, susceptibilities, and related quantities in the frequency domain. Our theory shows that the convolution inherent in a Fourier Neural Operator induces frequency coupling: even after spectral truncation, a reduced kernel retains energy at higher modes. The predicted behavior depends on whether the activation is analytic or has singular features, and the experiments confirm these theoretical patterns. The kernel-evolution formula we derived matches measured kernels across depths and widths, and the parallel and perpendicular susceptibilities observed under small perturbations fall well within the theoretical confidence intervals. Together, these results provide practical criteria for choosing hyper-parameters of the initialization ensemble.



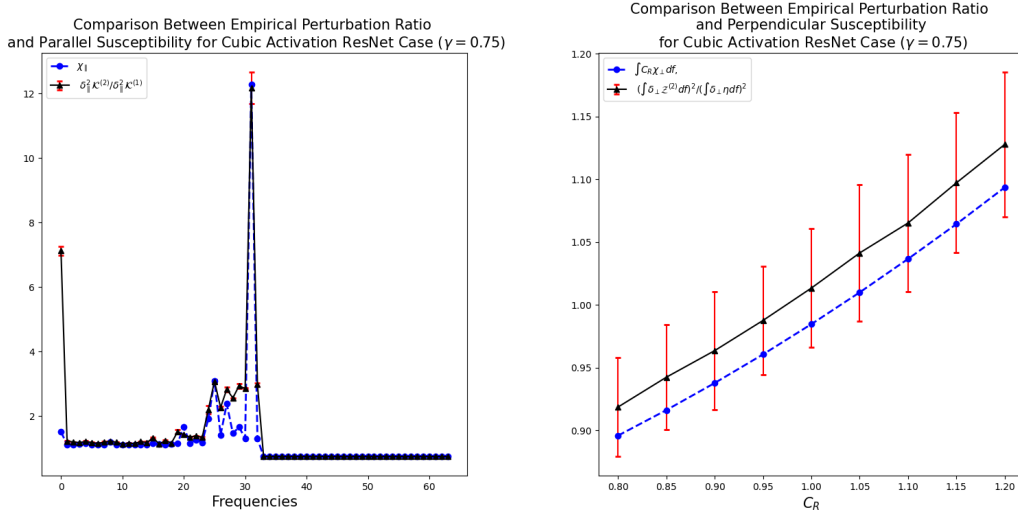


Figure 10: Comparison of empirical and theoretical susceptibility predictions for ReLU (top), and cubic activations with residual connection at $\gamma = 0.25$ (middle) and $\gamma = 0.75$ (bottom); red error bars show ± 1 standard deviation. (Left: parallel susceptibility, Right: perpendicular susceptibility)

Future work could develop concrete algorithms for setting those parameters, extend the analysis to activations beyond the analytic, scale-invariant, and residual cases treated here, track the evolution of the ensemble distribution during training, and investigate higher-order correlations.

Acknowledgments This work is supported by a KIAS Individual Grant (CG102201) at Korea Institute for Advanced Study and by the Center for Advanced Computation at Korea Institute for Advanced Study.

References

- I. Banta, T. Cai, N. Craig, and Z. Zhang. Structures of neural network effective theories. *Phys. Rev. D*, 109:105007, 2024.
- J. A. L. Benitez, T. Furuya, F. Faucher, A. Kratsios, X. Tricoche, and M. V. Hoop. Out-of-distributional risk bounds for neural operators with applications to the helmholtz equation. *Journal of Computational Physics*, 513:113168, 2024.
- G. Gupta, X. Xiao, and P. Bogdan. Multiwavelet-based operator learning for differential equations. *Advances in Neural Information Processing Systems*, 2021.
- J. Halverson, A. Maiti, and K. Stoner. Neural networks and quantum field theory. *Mach. Learn.: Sci. Technol.*, 2:035002, 2021.

M. Heydenreich and R. V. Hofstad. Functionals of brownian bridges arising in the current mismatch in d/a-converters. *Probability in the Engineering and Informational Sciences*, 23:149–172, 2009.

T. Kim and M. Kang. Bounding the rademacher complexity of fourier neural operators. *Machine Learning*, 113:2467–2498, 2024.

T. Koshizuka, M. Fujisawa, Y. Tanaka, and I. Sato. Understanding the expressivity and trainability of fourier neural operator: A mean-field perspective. *Proceedings of the Neural Information Processing Systems Conference (NeurIPS)*, 2024.

N. Kovachki, S. Lanthaler, and S. Mishra. On universal approximation and error bounds for fourier neural operators. *Journal of Machine Learning Research*, 22(290), 2021a.

N. Kovachki, Z. Li, B. Liu, K. Azizzadenesheli, K. Bhattacharya, A. Stuart, and A. Anandkumar. Neural operator: Learning maps between function spaces. *arXiv*, arXiv:2108.08481, 2021b.

Y. A. LeCun, L. Bottou, G. B. Orr, and KR Müller. *Efficient BackProp*. Springer, Berlin, 2002.

W. Lee, T. Kim, and H. Park. Fourier neural operators for non-markovian processes: Approximation theorems and experiments. *arXiv*, arXiv:2507.17887, 2025.

Z. Li, N. Kovachki, K. Azizzadenesheli, B. Liu, K. Bhattacharya, A. Stuart, and A. Anandkumar. Neural operator: Graph kernel network for partial differential equations. *ICLR 2020 Workshop ODE/PDE+DL*, 2020.

Z. Li, N. Kovachki, K. Azizzadenesheli, B. Liu, K. Bhattacharya, A. Stuart, and A. Anandkumar. Fourier neural operator for parametric partial differential equations. *ICLR 2021*, 2021.

L. Lu, P. Jin, G. Pang, Z. Zhang, and G. E. Karniadakis. Learning nonlinear operators via deeponet based on the universal approximation theorem of operators. *Nature Machine Intelligence*, 3:218–229, 2021.

J. Pathak, S. Subramanian, P. Harrington, S. Raja, A. Chattopadhyay, M. Mardani, T. Kurth, D. Hall, Z. Li, K. Azizzadenesheli, P. Hassanzadeh, K. Kashinath, and A. Anandkumar. Fourcastnet: A global data-driven high-resolution weather model using adaptive fourier neural operators. *arXiv*, arXiv:2202.11214, 2022.

C. E. Rasmussen. *Gaussian Processes in Machine Learning*. Springer, Berlin, 2004.

D. A. Roberts, S. Yaida, and B. Hanin. *The Principles of Deep Learning Theory*. Cambridge University Press, 2022.

A. Y. Sun, Z. Li, W. Lee, Q. Huang, B. R. Scanlon, and C. Dawson. Rapid flood inundation forecast using fourier neural operator. *IEEE/CVF International Conference on Computer Vision Workshops (ICCVW)*, 2023.

J. H. V. Vleck. *The Spectrum of Clipped Noise*. Harvard University, 1943.